

**THE IMPACT OF RIVER REHABILITATION ON  
FLOOD MITIGATION:  
A CASE STUDY OF ISMETIYE CREEK BURSA**

**Amir Iqbal WANI**



T.C.  
BURSA ULUDAĞ ÜNİVERSİTESİ  
FEN BİLİMLERİ ENSTİTÜSÜ

**THE IMPACT OF RIVER REHABILITATION ON FLOOD MITIGATION:  
A CASE STUDY OF ISMETIYE CREEK BURSA**

Amir Iqbal WANI  
0000-0001-6424-5697

Prof. Dr. Serdar KORKMAZ  
0000-0002-3393-1632  
(Danışman)

YÜKSEK LİSANS TEZİ  
İNŞAAT MÜHENDİSLİĞİ ANABİLİM DALI

BURSA – 2022  
**Her Hakkı Saklıdır**

## TEZ ONAYI

Amir Iqbal WANI tarafından hazırlanan “THE IMPACT OF RIVER REHABILITATION ON FLOOD MITIGATION: A CASE STUDY OF ISMETIYE CREEK BURSA” adlı tez çalışması aşağıdaki jüri tarafından oy birliği ile Bursa Uludağ Üniversitesi Fen Bilimleri Enstitüsü İnşaat Mühendisliği Anabilim Dalı’nda **YÜKSEK LİSANS TEZİ** olarak kabul edilmiştir.

**Danışman:** Prof. Dr. Serdar KORKMAZ

- Başkan** : Prof. Dr. Serdar KORKMAZ İmza  
0000-0002-3393-1632  
Bursa Uludağ Üniversitesi,  
Mühendislik Fakültesi,  
İnşaat Mühendisliği Anabilim Dalı
- Üye** : Prof. Dr. Fatma Olcay TOPAÇ İmza  
0000-0002-6364-4087  
Bursa Uludağ Üniversitesi,  
Mühendislik Fakültesi,  
Çevre Mühendisliği Anabilim Dalı
- Üye** : Doç. Dr. Babak VAHEDOOST İmza  
0000-0002-4767-6660  
Bursa Teknik Üniversitesi,  
Mühendislik ve Doğa Bilimleri Fakültesi,  
İnşaat Mühendisliği Anabilim Dalı

**Yukarıdaki sonucu onaylarım**

**Prof. Dr. Hüseyin Aksel EREN**  
**Enstitü Müdürü**

.././....

**B.U.Ü. Fen Bilimleri Enstitüsü tez yazım kurallarına uygun olarak hazırladığım bu tez çalışmada;**

- tez içindeki bütün bilgi ve belgeleri akademik kurallar çerçevesinde elde ettiğimi,
- görsel, işitsel ve yazılı tüm bilgi ve sonuçları bilimsel ahlak kurallarına uygun olarak sunduğumu,
- başkalarının eserlerinden yararlanılması durumunda ilgili eserlere bilimsel normlara uygun olarak atıfta bulunduğumu,
- atıfta bulunduğum eserlerin tümünü kaynak olarak gösterdiğimi,
- kullanılan verilerde herhangi bir tahrifat yapmadığımı,
- ve bu tezin herhangi bir bölümünü bu üniversite veya başka bir üniversitede başka bir tez çalışması olarak sunmadığımı

**beyan ederim.**

**18/04/2022**

**Amir Iqbal WANI**

**TEZ YAYINLANMA  
FİKRİ MÜLKİYET HAKLARI BEYANI**

Enstitü tarafından onaylanan lisansüstü tezin/raporun tamamını veya herhangi bir kısmını, basılı (kâğıt) ve elektronik formatta arşivleme ve aşağıda verilen koşullarla kullanıma açma izni Bursa Uludağ Üniversitesi'ne aittir. Bu izinle Üniversiteye verilen kullanım hakları dışındaki tüm fikri mülkiyet hakları ile tezin tamamının ya da bir bölümünün gelecekteki çalışmalarda (makale, kitap, lisans ve patent vb.) kullanım hakları tarafımıza ait olacaktır. Tezde yer alan telif hakkı bulunan ve sahiplerinden yazılı izin alınarak kullanılması zorunlu metinlerin yazılı izin alınarak kullandığını ve istenildiğinde suretlerini Üniversiteye teslim etmeyi taahhüt ederiz.

Yükseköğretim Kurulu tarafından yayınlanan “**Lisansüstü Tezlerin Elektronik Ortamda Toplanması, Düzenlenmesi ve Erişime Açılmasına İlişkin Yönerge**” kapsamında, yönerge tarafından belirtilen kısıtlamalar olmadığı takdirde tezin YÖK Ulusal Tez Merkezi / B.U.Ü. Kütüphanesi Açık Erişim Sistemi ve üye olunan diğer veri tabanlarının (Proquest veri tabanı gibi) erişimine açılması uygundur.

Serdar KORKMAZ  
18/04/2022

Amir Iqbal WANI  
18/04/2022

İmza

Bu bölüme kişinin kendi el yazısı ile okudum  
anladım yazmalı ve imzalanmalıdır.

İmza

Bu bölüme kişinin kendi el yazısı ile okudum  
anladım yazmalı ve imzalanmalıdır.

## ÖZET

Yüksek Lisans Tezi

### TAŞKINLA MÜCADELEDE NEHİR ISLAHININ ETKİSİ: BURSA İLİ İSMETİYE DERESİ UYGULAMASI

**Amir Iqbal WANI**

Bursa Uludağ Üniversitesi  
Fen Bilimleri Enstitüsü  
İnşaat Mühendisliği Anabilim Dalı

**Danışman:** Prof. Dr. Serdar KORKMAZ

Bu çalışmada, Bursa'da bulunan İsmetiye deresinde yapılmakta olan nehir ıslahının, taşkın yatağı haritası üzerindeki etkisi  $Q_{500}$  ve  $Q_{1000}$  debileri için incelenmiştir. Bunun için gerekli veriler kanal içi ve havzadaki yükseklik verileri ile debi değerleridir. ArcMap'de havzanın sayısal yükseklik modelini oluşturmak için hem nokta yükseklik verileri hem de topografik kontur çizgileri kullanılmıştır. Daha sonra bu model, HEC-RAS programı kullanılarak, havzanın ekstrem debiler altında taşkın yatağı haritasının çıkarılmasında kullanılmıştır. Taşkın yatağı haritası, nehrin ıslah edilmesinden önce ve sonra olmak üzere her iki durum için de oluşturulmuştur. Daha sonra bu iki durum için su derinliği ve taşkın haritaları karşılaştırılmıştır. Buna ek olarak, taşkın tehlike haritaları, taşkın hız haritaları ve su yüzeyi yükseklik haritaları çizilip karşılaştırılmıştır. Nehir boyunca belirlenen istasyonlarda ana kanaldaki ve taşkın yataklarındaki akım hidrografları hesaplanmıştır. Islah çalışmalarının, taşkın yatağı akımını ve taşkın yayılımını önemli ölçüde azaltarak taşkınla mücadeleye katkıda bulunduğu görülmüştür. Son olarak, ilerideki çalışmalar için bazı öneriler sunulmuştur.

**Anahtar Kelimeleri:** nehir ıslahı, taşkın yatağı haritası, taşkın tehlikesi, HEC-RAS  
**2022, ix + 62 sayfa.**

## **ABSTRACT**

MSc Thesis

### **THE IMPACT OF RIVER REHABILITATION ON FLOOD MITIGATION: A CASE STUDY OF ISMETIYE CREEK BURSA**

**Amir Iqbal WANI**

Bursa Uludağ University  
Graduate School of Natural and Applied Sciences  
Department of Civil Engineering

**Supervisor:** Prof. Dr. Serdar KORKMAZ

In this study, the impact of channel rehabilitation on the extent of floodplain map for  $Q_{500}$  and  $Q_{1000}$  discharges is investigated in the Ismetiye creek, located in Bursa, Turkey. The necessary data used is discharge and the elevation data for the main channel and the catchment area of Ismetiye creek. Both point elevation data and topographic contour lines are used to create the digital elevation model of the area in Arc Map. Subsequently, it is used to develop the floodplain model of catchment area for extreme discharges using HEC-RAS software for the two cases including before and after the rehabilitation of Ismetiye creek. Water depths and floodplain maps are compared for these two cases. In addition, flood hazard maps, flood velocity maps, and water surface elevation maps are developed and compared. Flow hydrographs in the main channel and overbanks are computed at specified stations along the river. It is observed that rehabilitation works contributed the flood mitigation by reducing overbank flows and flood extent considerably. Finally, some recommendations are proposed for future works.

**Keywords:** river rehabilitation, floodplain map, flood hazard, HEC-RAS  
**2022, ix + 62 pages.**

## **ACKNOWLEDGEMENT**

I want to express my gratitude towards Prof. Dr. Serdar KORKMAZ, without whose expertise and continuous guidance, this thesis work would not have been possible at all. I am also in debt towards my university in general and my department in particular for providing me with a nice working environment and all the necessary facilities that helped me in doing this study.

Besides, I would like to express my acknowledgement towards Bursa Su ve Kanalizasyon Idaresi (BUSKI) for providing all the necessary data used in carrying out this work. Last but not least, I would also like to sincerely thank my family and friends who have provided tremendous moral support to me during my study.

Amir Iqbal WANI  
18/04/2022

## TABLE OF CONTENTS

	<b>Page</b>
ÖZET.....	i
ABSTRACT.....	ii
ACKNOWLEDGEMENT.....	iii
LIST OF FIGURES.....	vii
LIST OF TABLES.....	vii
1. INTRODUCTION.....	1
1.1. General Introduction.....	1
1.2. Research Objectives.....	3
1.3. Scope of Study.....	3
1.4. Outline of Thesis.....	3
2. LITERATURE REVIEW.....	5
3. MATERIAL AND METHOD.....	10
3.1. Study Area.....	10
3.1.1. Climate and water resources.....	14
3.1.2. Meteorological data.....	14
3.2. Methodology.....	15
3.2.1. Flood discharge calculation.....	15
3.2.2. Topographic data preparation in ArcGIS.....	17
3.2.3. HEC-RAS.....	25
3.2.4. 2D-modelling in HEC-RAS.....	26
4. RESULTS AND DISCUSSION.....	36
4.1. Results of 2D Simulation Before Rehabilitation of Ismetiye Creek.....	36
4.2. Results of 2D Simulation After Rehabilitation of Ismetiye Creek.....	37
4.3. Comparison of results before and after the rehabilitation of Ismetiye creek.....	39
5. CONCLUSION.....	57
5.1. Summary and Conclusion.....	57
5.2. Recommendations.....	58
REFERENCES.....	60

## SYMBOLS AND ABBREVIATIONS

<b>Symbol</b>	<b>Definition</b>
A	Area
C	Courant Number
E	East
g	Gravitational Acceleration
N	North
q	inflow
Q	Discharge
S	Ineffective flow area
S <sub>f</sub>	Frictional Slope
T	Time
V	Velocity
X	Distance
Z	Elevation
Δx	Average Cell Size
Δt	Average Comptational Time

<b>Abbreviation</b>	<b>Definition</b>
1D	One Dimensional
2D	Two Dimensional
BC	Boundary Condition
BUSKI	Bursa Su ve Kanalizasyon İdaresi
CAD	Computer-aided Design
DEM	Digital Elevation Model
DSI	Devlet Su Isleri
DTM	Digital Terrain Model
ED	European Datum
EPA SWMM	Environmental Protection Agency's Stormwater Management Modelling
FEMA	Federal Emergency Management Agency
GIS	Geographic Information Systems
HBV Model	Hydrologiska Byrans Vattenbalansavdelning Model
HEC-HMS	Hydrologic Engineering Centre's Hydrologic Modelling System
HEC-RAS	Hydrologic Engineering Centre's River Analysis System
IDW	Inverse Distance Weighted
LiDAR	Light Detecting and Ranging
LOB	Left Overbank
MC	Main Channel
MOUSE	Modelling of Urban Drainage and Sewer
RIDF	Rainfall Intensity Duration Frequency
ROB	Right Overbank

SAR	Synthetic Aperture Radar
SRTM	Shuttle Radar Topography Mission
SWE	Shallow Water Equation
TOP Model	Topographic model
UTM	Universal Transverse Mercator
VIC	Variable Infiltration Capacity
WMS	Watershed Modelling
WSE	Water Surface Elevation

## LIST OF FIGURES

	<b>Page</b>
Figure 3.1.	Map showing Demirtas dam, Ismetiye creek (marked in blue) and the rehabilitated part (marked in green) of channel ..... 11
Figure 3.2.	Ismetiye creek in its natural state (BUSKI Report, 2013) A) downstream view at the end of Ismetiye village B) upstream view inside Ismetiye village ..... 12
Figure 3.3.	Ismetiye creek in its rehabilitated state A) downstream view at the end of Ismetiye village at X =3500 m B) upstream view inside Ismetiye village at X=2500..... 12
Figure 3.4.	Ismetiye creek in its rehabilitated state A) upstream view at 75 m B) upstream view at 4020 m ..... 13
Figure 3.5.	Downstream view of Ismetiye creek at 4020 m..... 23
Figure 3.6.	Methodology adopted to perform the flood simulations in this study. 15
Figure 3.7.	Shows the CAD data as it is imported to ArcMap..... 18
Figure 3.8.	Point elevation data of Ismetiye channel and surrounding areas ..... 19
Figure 3.9.	Point elevation data of Ismetiye channel and surrounding areas after inserting additional points in ArcMap..... 20
Figure 3.10.	DEM of resolution 0.5m as obtained from IDW raster interpolation method in Arc Map ..... 21
Figure 3.11.	Intermediate sections in the concrete channel with 20-m intervals ... 22
Figure 3.12.	Point elevation data with concrete channel..... 23
Figure 3.13.	DEM of the rehabilitated channel ..... 24
Figure 3.14.	Setting projection to the RAS Mapper file..... 28
Figure 3.15.	Adding terrain to the RAS Mapper file ..... 28
Figure 3.16.	Adding a new modification layer to the RAS Mapper file ..... 29
Figure 3.17.	Terrain in RAS Mapper A) before modification B) after modification ..... 29
Figure 3.18.	Adding geometry of the channel in RAS Mapper ..... 30
Figure 3.19.	Editing geometry to define flow area in RAS Mapper ..... 30
Figure 3.20.	Defining the mesh size in RAS Mapper ..... 31
Figure 3.21.	Flow area showing A) boundary conditions B) mesh size of 10 m x10 m..... 31
Figure 3.22.	Refinement of 2D mesh in RAS Mapper by using ‘breaklines’..... 32
Figure 3.23.	Refinement of 2D mesh in RAS Mapper by using ‘breaklines’..... 32
Figure 3.24.	Assigning Manning’s n value to the concrete channel and overbanks 33
Figure 3.25.	Importing the RAS Mapper file to HEC-RAS geometry ..... 34
Figure 3.26.	Adding flow hydrograph and friction slope to boundary conditions... 34
Figure 3.27.	Performing unsteady flow simulation ..... 35
Figure 4.1.	Case 1: Flood map for Q500 before rehabilitation A) HEC-RAS terrain view B) Google satellite view ..... 36
Figure 4.2.	Case 2: Flood map for Q1000 before rehabilitation A) HEC-RAS terrain view B) Google satellite view ..... 37
Figure 4.3.	Case 3: Flood map for Q500 after rehabilitation A) HEC-RAS terrain view B) Google satellite view ..... 38
Figure 4.4.	Case 4: Flood map for Q1000 after rehabilitation A) HEC-RAS terrain view B) Google satellite view ..... 38

Figure 4.5.	The comparison of flood maps for Q500 A) before rehabilitation B) after rehabilitation .....	39
Figure 4.6.	The comparison of flood maps for Q1000 A) before rehabilitation B) after rehabilitation .....	40
Figure 4.7.	Velocity maps for Q500 A) before rehabilitation B) after rehabilitation .....	41
Figure 4.8.	Velocity maps for Q1000 A) before rehabilitation B) after rehabilitation .....	42
Figure 4.9.	Water Surface Elevation maps for Q500 A) before rehabilitation B) after rehabilitation .....	43
Figure 4.10.	Water Surface Elevation maps for Q1000 A) before rehabilitation B) after rehabilitation .....	44
Figure 4.11.	Flood hazard zones for Q500 A) before rehabilitation B) after rehabilitation .....	45
Figure 4.12.	Flood hazard zones for Q1000 A) before rehabilitation B) after rehabilitation .....	47
Figure. 4.13.	Cross-sections at X=75 m for Q1000 A) before rehabilitation B) after rehabilitation .....	48
Figure 4.14.	Flow hydrographs for Q500 at X=75 m for main channel and overbanks .....	49
Figure 4.15.	Flow hydrographs for Q1000 at X=75 m for main channel and overbanks .....	49
Figure 4.16.	Cross-sections at X=1500 m for Q1000 A) before rehabilitation B) after rehabilitation .....	50
Figure 4.17.	Flow hydrographs for Q500 at X=1500 m for main channel and overbanks .....	50
Figure 4.18.	Flow hydrographs for Q1000 at X=1500 m for main channel and overbanks .....	51
Figure 4.19.	Cross-sections at X= 3000 m for Q1000 A) before rehabilitation B) after rehabilitation.....	52
Figure 4.20.	Flow hydrographs for Q500 at X=3000 m for main channel and overbanks .....	52
Figure 4.21.	Flow hydrographs for Q1000 at X=3000 m for main channel and overbanks .....	53
Figure 4.22.	Cross-sections at X=4000 m for Q1000 A) before rehabilitation B) after rehabilitation .....	53
Figure 4.23.	Flow hydrographs for Q500 at X=4000 m for main channel and overbanks.....	54
Figure 4.24.	Flow hydrographs for Q1000 at X=4000 m for main channel and overbanks .....	54

## LIST OF TABLES

	<b>page</b>
Table 1.1. Catastrophic flood events with high (>30) fatality numbers in Turkey from 1930 to 2021 (Modified from Haltas et al.,2020) .....	1
Table 1.2. Summary of losses due to flood events in Turkey 1930-2020 (Haltas et al.,2020).....	2
Table 3.1. Project area meteorology stations (BUSKI Report, 2013).....	14
Table 3.2. Q500 and Q1000 in the Ismetiye creek for a 20-hour hydrograph (BUSKI Report, 2013).....	16
Table 4.1. Flood risk classification scheme (modified from FEMA 2018).....	45
Table 4.2. Peak discharge values for natural and concrete channels in case of Q500.....	55
Table 4.3. Peak discharge values for natural and concrete channels in case of Q1000.....	55

# 1. INTRODUCTION

## 1.1. General Introduction

Flood can be defined as water overflowing a usually dry land resulting in submerging of the land. Floods are the most frequent type of natural disaster. They are often caused by heavy rainfall, rapid snowmelt or a storm surge from a tropical cyclone or tsunami in coastal areas. Even though the loss to life due to flood events during the past century has declined, the economic losses due to floods have continued to rise. This is due to the increase in urbanization and coastal development (WHO 2022).

Turkey experienced rapid urbanization during the past years which is why Turkey is still unprepared for many natural disasters including floods. Table 1.1 shows the most catastrophic flood events in Turkey from 1930-2021.

**Table 1.1.** Catastrophic flood events with high (>30) fatality numbers in Turkey from 1930 to 2021 (Modified from Haltas et al.,2020)

Event Date	Province	Fatality
09-11-1957	Ankara	165
03-06-1948	Amasya	92
13-07-1995	Isparta	74
11-08-2021	Kastamonu	62
04-11-1995	İzmir	61
28-03-1980	Kayseri	60
24-10-1930	İzmir	40
08-09-2009	İstanbul	31

In Turkey, floods are the second most destructive types of natural disasters. 30% of natural disaster constitute of floods. Flash floods caused by prolonged and severe rainfalls are commonly observed especially in coastal regions of Turkey. Flood impacts are felt more strongly in Turkey's largest cities, which suffer from regular floods as a consequence of the combined effects of extreme rainfall, residential and commercial usage of flood plain and poor drainage. Since 1970, a flash flood prevention program has been successful in lowering the number of flash floods. However, significant structural and mitigation work are still required, particularly in metropolitan regions of the nation,

to prevent flash floods and mitigate their effects (Climate Change Post, 2022). Table 1.2 shows summary of losses due to flood events in Turkey from 1930 to 2020.

**Table 1.2.** Summary of losses due to flood events in Turkey 1930-2020 (Haltas et al.,2020)

Risk Factor	Events	Ratio (%)	Total Loss	Loss per Event
Fatality	206	9.8	1026	4.98
Injury	79	3.8	402	5.09
Flooded Unit	539	25.8	64930	120.46
Destroyed Property	70	3.3	709	10.13
Flooded Vehicle	48	2.3	1485	30.94
Perished Cattle	34	1.6	2504	73.65
Perished Ovine	54	2.6	14123	261.54
Flooded Agri.Land (sqm)	71	3.4	1736	24.45
Direct Econ. Loss (M TL)	56	2.7	2160	38.57

Bursa, which is an industrial hub in the North-Western Turkey, is no exception. It is also affected by floods time to time. Bursa has experienced many floods during the past 3 decades. Recently in the month of June 2020, flash floods killed 5 people in Kestel, a district 30 Km's from central Bursa. The flash flood was caused by heavy downpours, leaving the villages inundated by floodwaters. Before that, the most fatal floods seen in Bursa were 1989 floods in Setbasi Gokdere, 2001 floods again in Setbasi Gokdere, 2005 floods in Yildirim Hacivat and Delicay stream, and 2010 floods in Cilimboz stream (Bursa Haber 2010).

The population of Bursa increased from 148.000 in 1950 to 3 million in 2020 (Macrotrends, 2020). This caused increase in the demand for city's water resources. This stress is further accompanied by global warming impacts. These impacts include high precipitation rates and rising sea water levels for low-lying coastal areas. As a result of such local variations in the hydrological cycle, there is an increased need for more accurate predictions of hydrologic models. Flooding is also a threat in the river bank areas of Bursa. Hence a reliable hydrologic model is required to predict the flood levels in light of a flood event.

## **1.2. Research Objectives**

This research project aims at:

- Conducting a literature review for the current studies involving floodplain modelling by using HEC-RAS and some other software.
- Developing digital elevation model (DEM) of the study area in ArcMap for both natural and rehabilitated states of Ismetiye creek and using this model for developing a floodplain model of the catchment area for extreme discharges in HEC-RAS.
- Comparing the results before and after the rehabilitation of Ismetiye creek and analysing the impact of rehabilitation work on flood mitigation.
- Giving necessary suggestions based on the results of this study for further improvement of flood mitigation works.

## **1.3. Scope of Study**

BUSKI has been carrying out rehabilitation works in urban areas in Bursa. In this research, the impact of rehabilitation of Ismetiye creek on the flood mitigation in Ismetiye catchment area in Bursa was studied through 2D flood modelling. Necessary data used in this study was elevation data and discharge, both collected from BUSKI. Using the elevation data, ArcMap was used to create DEM of the study area. This DEM was then exported to HEC-RAS to develop 2D floodplain models for  $Q_{500}$  and  $Q_{1000}$ . These models were developed for both before and after creek rehabilitation. Eventually, the developed models were analysed and compared to study the impact of creek rehabilitation on flood mitigation.

## **1.4. Outline of Thesis**

The thesis consists of five chapters. Chapter one is the Introduction. Chapter two encompasses the Literature Review, summarising previous academic studies on the subject using HEC-RAS and other software. Chapter three Material and Method gives

details about methodology followed, software and data used. In the fourth chapter Results and Discussion, findings of the study are presented. In the fifth chapter Conclusion, obtained results are explained, interpreted and necessary suggestions are proposed.

## 2. LITERATURE REVIEW

In this chapter, different studies for doing flood plain modelling by using HEC-RAS and other software were reviewed. Apart from this, research works showing impact of river rehabilitation on flood mitigation were also investigated.

Tahmasbinejad et al. (2012) developed a regional scale flood modelling integrating HEC-RAS and HEC-HMS with GIS to simulate relations between rainfall and runoff in Karun River, Iran. They obtained overland flow and channel runoff from precipitation by using HEC-HMS and then derived hydrographs. HEC-RAS was used to model unsteady-state flow through the river channel network. They found out Log-Pearson III as the best distribution to estimate peak flow for different return periods. They also found out that SCS method gave better results for runoff estimation in ungauged catchments compared to the Snyder method. HEC-RAS model was used in simulating flow depth in different parts of the floodplain.

Iglesias (2014) studied the flood disaster mitigation and river rehabilitation of Marikina River banks in Philippines. The river banks were rebuilt keeping in consideration the flood risk. Apart from this, regular river dredging was carried out to get rid of the debris in the river. The results showed that there was a considerable decrease in the area of land flooded during 2004 floods as compared to the area of land flooded during 1992 floods.

Liu et al. (2014) studied the effect of river rehabilitation on flood reduction in the Alzette River Basin, Luxemburg. Some rehabilitation measures carried out are changing riparian, in-stream vegetation and planting. As a result of the rehabilitation, it was observed that a reduction in peak flow by an amount of 14% occurred and the time of concentration was also delayed by two hours. They concluded that river rehabilitation has a good influence in decreasing the risk of flooding downstream.

Hashemyan et al. (2015) investigated the behaviour of river flood by the integration of HEC-HMS hydrological and HEC-RAS hydraulic model. Flood zones associated with precipitation periods of 10, 20, 50 and 100 years were determined by using HEC-GeoRAS

extension in GIS environment. Curve Number method was used to convert rainfall into runoff. The precipitation of return periods 10, 20, 50 and 100 years was extracted from intensity-duration-frequency curves. Additionally, flood hydrograph was computed for various return periods using HEC-RAS software. The best statistical distribution of discharges using Hyfa software was found as Pearson Type III.

Astite et al. (2015) used cartography of flood hazards to manage the flood risk. They used HEC-RAS as well as Arc-GIS to develop the cartography. Water depths of different peak flows were calculated. Hydraulic modelling results combined with land-use under Arc-GIS were used to develop flood hazard maps with different frequencies (T10, T20, T50, T100 and T200). The cartography was aimed at helping develop a prevention plan against inundations for the management and the urbanization planning.

Yamani et al. (2016) did vulnerability mapping of flood areas in Ghardia. The aim was to develop a risk prevention plan for flooding. Two types of models were tested. Hydrological model HEC-HMS and the hydraulic model HEC-RAS. As a result, the water profile was plotted in the HEC-RAS software. It was noted that the heights of water level obtained by simulation are very close to the real values. Eventually, vulnerability zones were pointed out.

Bricker et al. (2017) applied the 1-dimensional HEC-RAS model for downstream flood routing in the Kali Gandaki River of Nepal and then compared it to the 2-dimensional Delft-FLOW model. It was concluded that a 2-dimensional model produces more accurate results. Thus, 2-dimensional model was recommended for hazard assessment and planning. On the other hand, a 1-dimensional model was found to be more suitable for facilitating real-time warning declaration.

Thakur et al. (2017) evaluated the extent of flood plain utilizing a known precipitation and land use. HEC-HMS was used as a modelling tool to develop runoff and HEC-RAS was used to develop a floodplain inundation model for known precipitation. A rainfall-runoff model was developed to achieve the flood inundation extent for the known

precipitation event. The results of simulated runoff for the precipitation event were achieved in HEC-HMS and floodplain model was generated in HEC-RAS.

Acosta et al. (2017) used HEC-RAS and HEC-HMS to generate GIS flood models aimed at simulating flood inundation. They used SAR (Synthetic Aperture Radar) and Digital Terrain Model (DTM) derived from Light Detecting and Ranging (LiDAR) datasets. As an input for the setup of HEC-RAS model, 24 hour 5-year, 25-year and 100-year Rainfall Intensity Duration Frequency (RIDF) curves were used. Three simulations with 5-year, 25-year and 100-year return periods were done. Flood inundation maps of the study area were generated. Eventually, HEC-RAS flood was used to calculate water levels.

Mondal and Patel (2017) reviewed some ecological techniques of flood and channel management. They concluded in their studies that that these ecological techniques such as floodplain and channel connectivity restoration are deemed more important than structural river engineering for the rehabilitation. However, these techniques are generally not applied in developing countries where the economic resources are scarce.

Şahin (2018) estimated flood inundated areas caused by failure of Urkmez dam in Izmir by using HEC-RAS one-dimensional and two-dimensional model. The risk of dam failure was analysed by comparing the two models. Simulations showed that areas submerged were approximately same for both cases but the estimated size of inundated area was around 5% larger in case of 2D simulations. It was also noted that the depth observed in one-dimensional simulation results was higher than that in two-dimensional simulation results, at the same time. However, the time to reach maximum velocity was lower in the two-dimensional model.

Abdessamed and Abderrazak (2019) analysed the inundation behaviour of Ain Sefra city during extreme flood events by considering concrete retaining walls built by local authorities and without it. In this case, three types of simulations were performed with the return periods of 10, 100, and 1000 years. Digital elevation models (DEMs) with 30 m resolution sourced from Shuttle Radar Topographic Mission (SRTM) were used. By

hydraulic modelling it was revealed that the existence of retaining walls would result in decrease of flood zone area.

Gulbaz et al. (2019) generated a hydrodynamic model of a watershed by using the Watershed Modelling System (WMS) (version 9.1) and the US Environmental Protection Agency's Storm Water Management Model (EPA SWMM). EPA SWMM model was used to calculate the flood depth and volume belonging to the flood event. In addition, flood hazard map was produced by using WMS.

Sammen et al. (2019) studied the environmental consideration in flood mitigation and river restoration in Malaysia. This study particularly emphasized on utilizing eco-friendly materials for achieving flood mitigation goals. The various steps taken were installing stakes to protect the river bank from erosion, protecting the banks using natural vegetation cover, scouring of river bank etc. It was concluded that these steps helped to restore rivers to their natural habitat.

Neslihan and Asli (2020) did the flood hazard assessment of an intensively flood-prone urbanized area in Samsun, Turkey. The program used for flood hazard assessment was MIKE FLOOD. Extent of flood, depth of flood and flood hazard were successfully shown in the modelling results. It was concluded that the local government bodies could use the results of the study in developing strategies to avoid flooding of the study area.

Natarajan et al. (2020) first discussed the causes of urban floods and then assessed the appropriate flood modelling methods that can be effectively used for urban catchments. Different flood modelling software were studied. These are HEC-RAS, HEC-HMS, TOP Model, MIKE SHE, HBV Model, SWAT, VIC (Variable Infiltration Capacity) Model, Stormwater Management Model, MOUSE (Modelling of Urban Drainage and Sewer) Model and MIKE-11 Model.

Anju et al. (2021) used MIKE FLOOD, a platform that combines Mike 11 and Mike 21 models into a single modelling frame to simulate flood inundation extent and water levels

at different locations of a river. The flood depth and water level at different locations of the river was obtained, and the extent of flood was simulated.

### **3. MATERIAL AND METHOD**

#### **3.1. Study Area**

The catchment area is located in the 1/25000 scaled maps H22-A4 and H22-D1 of Marmara Region, Bursa. The area is located between 29°7'0"E-40°17'30"N and 29°4'30"E-40°14'30"N geographic coordinates. The area of the catchment around Ismetiye Creek is 52.44 Km<sup>2</sup>. Figure 3.1 shows a satellite view of the Demirtaş dam, Ismetiye creek and the Ismetiye region settlements. Ismetiye creek originates from Demirtaş dam and joins with Nilüfer river in the south. Basin area is generally covered with forests and agricultural lands but there also are some residential areas in the south. Demirtaş dam, which was put into operation in 1983, is located at the upstream of Ismetiye creek. The water source of Demirtaş dam is Ballık stream. Ballık stream arises at an elevation of 1000 m, flows westward and reaches Demirtaş dam at an elevation of 170 m. Demirtaş dam spillway outflow and Ismetiye creek intermediate basin flow cause potential floods for which the channel was rehabilitated. The length of Ismetiye creek (shown in blue) is 8140 m and the length of rehabilitated channel (shown in green) is 4020 m. Slope of Ismetiye channel in its natural state was 0.006. As per the Rosgen Level I Stream Classification Technique (Rosgen, 1994), the channel has a gentle slope (<2%). Thus, it can be classified as 'C Stream Type'.

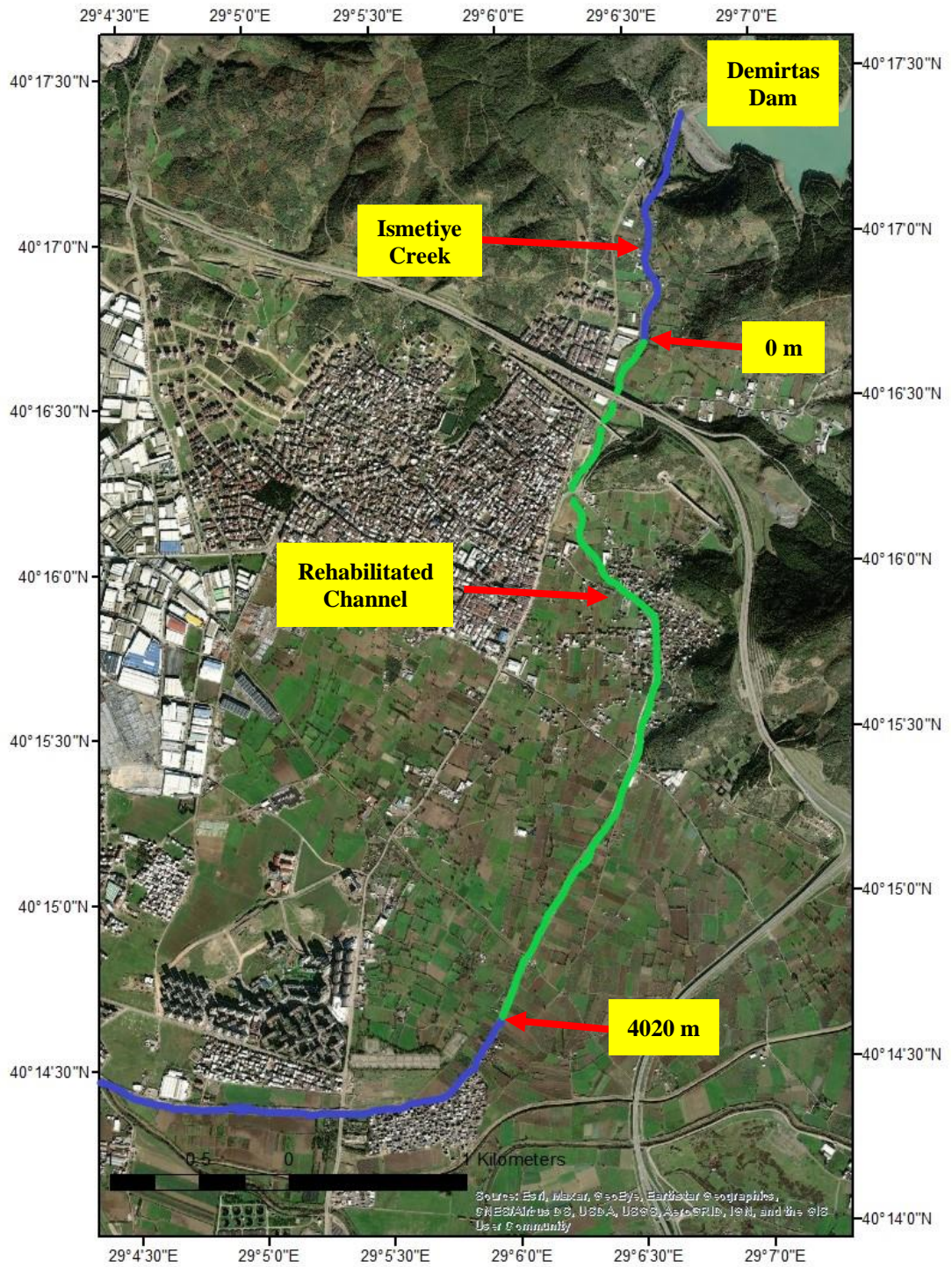


**Figure 3.1.** Map showing Demirtas dam, Ismetiye creek (marked in blue) and the rehabilitated part (marked in green) of channel.

Ismetiye creek, in its natural state before rehabilitation, was more prone to flood risk. Figure 3.2 shows Ismetiye creek in its natural state.

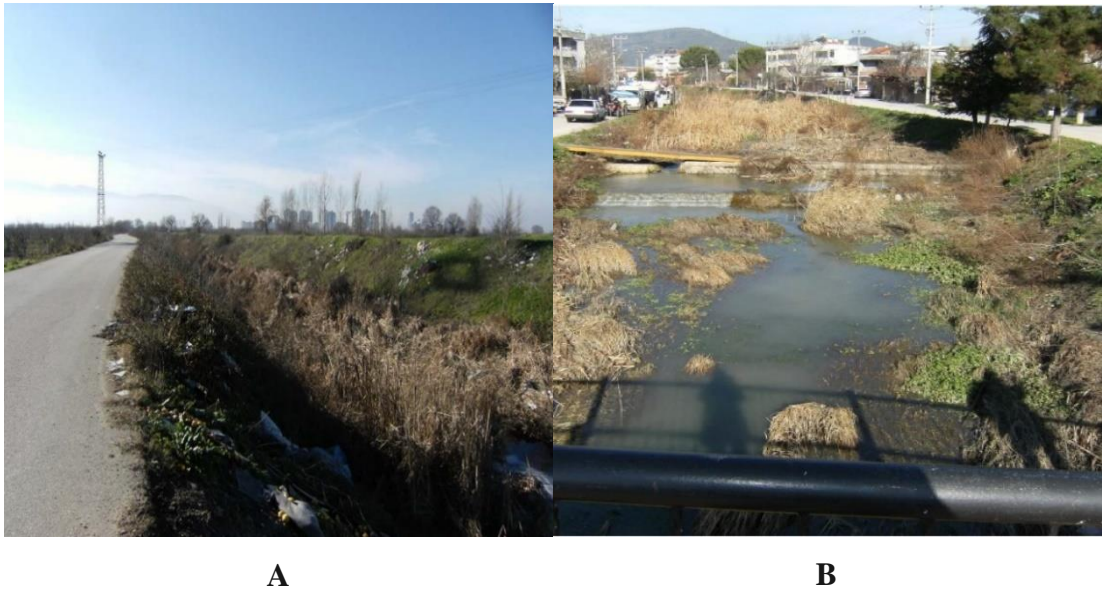


**Figure 3.2.** Ismetiye creek in its natural state (BUSKI Report, 2013) **A)** downstream view at the end of Ismetiye village **B)** upstream view inside Ismetiye village

The rehabilitation work was started by BUSKI in the year 2013 and finished in 2017. Figure 3.3 shows Ismetiye creek in its rehabilitated state as of March, 2022.

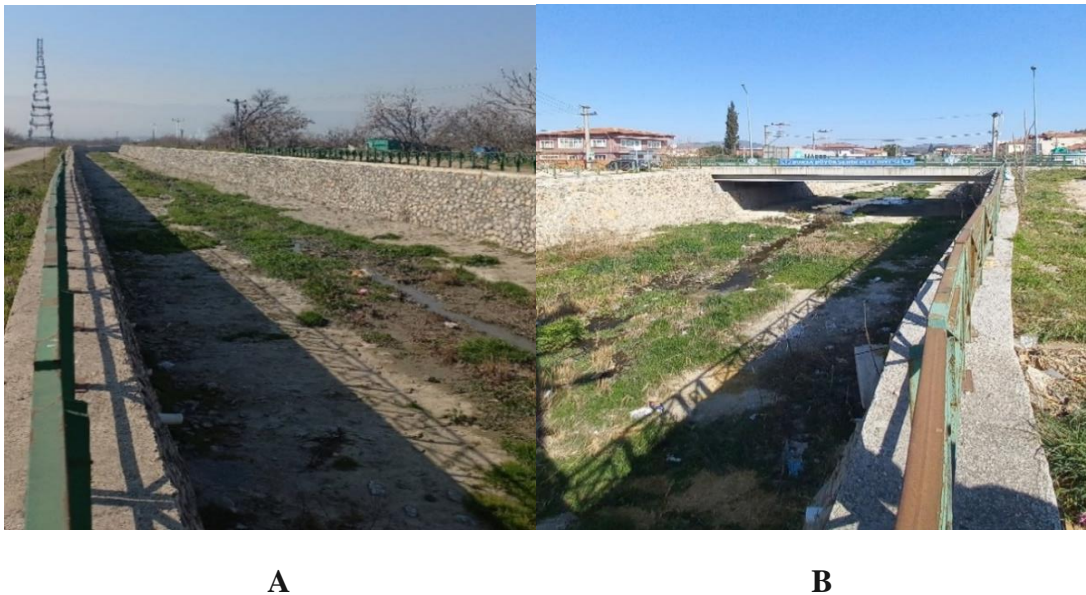


**Figure 3.3.** Ismetiye creek in its rehabilitated state **A)** downstream view at the end of Ismetiye village at X =3500 m **B)** upstream view inside Ismetiye village at X= 2500 m

Figure 3.4 shows Ismetiye creek at the beginning and end points of rehabilitation



**A**

**B**

**Figure 3.4.** Ismetiye creek in its rehabilitated state **A)** upstream view at 75 m **B)** upstream view at 4020 m

Figure 3.5 shows Ismetiye creek in its natural state as seen from the spot where rehabilitation work was stopped.



**Figure 3.5.** Downstream view of Ismetiye creek at 4020 m

### 3.1.1. Climate and water resources

The study area, Bursa, which is in the Marmara region of Turkey, is a transition zone between Mediterranean climate and Black Sea climate. In this climate, winters are cold or cool, snowy from time to time, summers are hot and dry. The factors affecting climate of the project area are elevation from the sea level, mountain ranges nearby reducing the warming effect from the sea and cold weather currents originating from the Balkan region.

### 3.1.2. Meteorological data

Meteorological stations located in the project area, their observations and time periods, and station locations are shown in Table 3.1. The base station in the project area is the Bursa meteorology station (State Meteorological Service). All kinds of meteorological observations (precipitation, temperature, evaporation, humidity, wind, etc.) are made at this station.

**Table 3.1. Project area meteorology stations (BUSKI Report, 2013)**

Station Name	Survey Period	Operating Department	Station Altitude (m)	Observations made			
				Rain	Temp.	Wind	Moisture
Bursa Meteorological Station	1929-2012	State Meteorological Service	100	+	+	+	+

The annual average precipitation for the project area from 1929 to 2012 observed is 675 mm. The maximum daily rainfall recorded in the observation period from 1929 to 2012 is 200 mm which was recorded in July 1942. The annual average temperature at Bursa Meteorology Station is 14.40 °C. The minimum observed temperature is -25.7 °C and maximum observed temperature is 42.6 °C. The annual average humidity as recorded at Bursa meteorology station is 69 %. The monthly average wind speed recorded at the station is 3 m/s in winter and 2.5 m/s in spring and summer.

### 3.2. Methodology

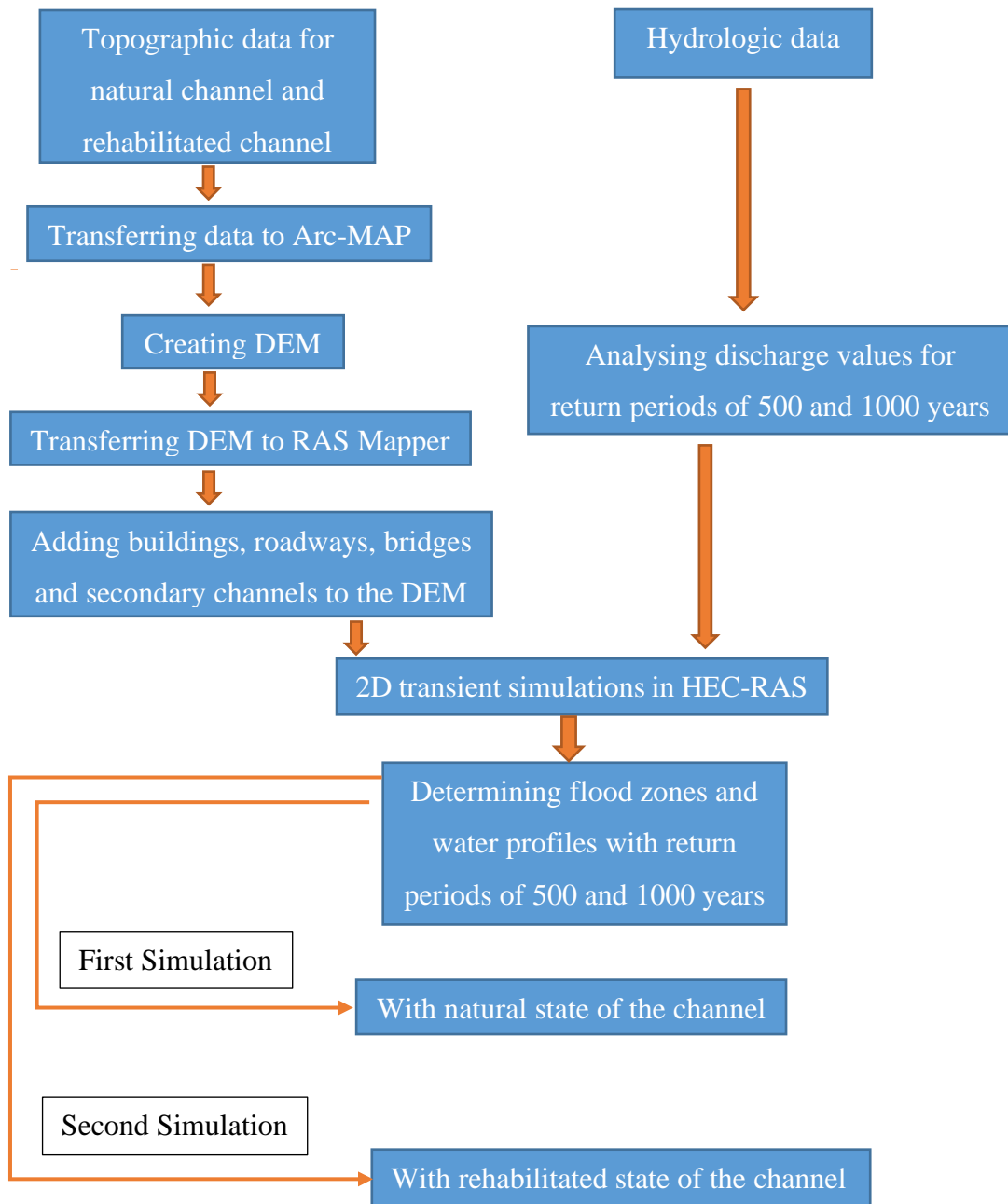


**Figure 3.6.** Methodology adopted to perform the flood simulations in this study

#### 3.2.1. Flood discharge calculation

In the calculation of design flow through the channel, two methods namely Mockus Method and DSI Synthetic Method were used by BUSKI in their report, keeping in view

the project criteria and technical specifications deemed right by the State Hydraulic Works Department (DSI).

The results obtained from both Mockus and DSI Synthetic method were compared in the BUSKI report, 2013. However, the results obtained from DSI Synthetic method were accepted and used for the design of rehabilitation channel.  $Q_{500}$  and  $Q_{1000}$  values as obtained from the DSI Synthetic method for a 20-hour hydrograph can be seen in Table 3.2.

**Table 3.2.**  $Q_{500}$  and  $Q_{1000}$  in the Ismetiye creek for a 20-hour hydrograph (BUSKI Report, 2013)

DEMIRTAS DAM SPILLWAY FLOW			ISMETIYE INTERMEDIATE BASIN FLOW		AFTER SUPERPOSITION TOTAL FLOW	
T	$Q_{500}$	$Q_{1000}$	$Q_{500}$	$Q_{1000}$	$Q_{500}$	$Q_{1000}$
(Hour)	( $m^3/s$ )	( $m^3/s$ )	( $m^3/s$ )	( $m^3/s$ )	( $m^3/s$ )	( $m^3/s$ )
0.0	0.00	0.00	0.00	0.00	0.00	0.00
0.5	2.94	3.52	6.77	7.82	9.72	11.34
1.0	11.15	13.33	24.97	28.83	36.12	42.16
1.5	23.72	28.36	51.00	58.89	74.72	87.25
2.0	41.14	49.19	69.00	79.68	110.14	128.87
2.5	62.52	74.64	66.12	76.35	128.63	150.99
3.0	83.58	99.52	54.01	62.37	137.59	161.89
3.5	100.66	119.48	39.27	45.35	139.93	164.83
4.0	114.51	135.39	28.35	32.74	142.87	168.13
4.5	122.90	144.61	20.83	24.05	143.73	168.66
5.0	128.25	150.19	15.06	17.39	143.31	167.58
5.5	129.67	151.19	10.70	12.35	140.36	163.54
6.0	128.25	148.90	7.57	8.74	135.82	157.64
6.5	125.75	145.48	5.54	6.39	131.29	151.87
7.0	122.75	141.54	4.20	4.85	126.94	146.39
7.5	118.83	136.65	2.97	3.43	121.80	140.09
8.0	114.13	130.94	2.15	2.48	116.27	133.41

**Table. 3.1.**  $Q_{500}$  and  $Q_{1000}$  in the Ismetiye creek for a 20-hour hydrograph (continued)

DEMIRTAS DAM SPILLWAY FLOW			ISMETIYE INTERMEDIATE BASIN FLOW		AFTER SUPERPOSITION TOTAL FLOW	
T	$Q_{500}$	$Q_{1000}$	$Q_{500}$	$Q_{1000}$	$Q_{500}$	$Q_{1000}$
(Hour)	$m^3/s$	$m^3/s$	$m^3/s$	$m^3/s$	$m^3/s$	$m^3/s$
8.5	109.59	125.43	1.58	1.83	111.17	127.26
9.0	105.81	120.84	1.13	1.30	106.94	122.15
10.5	94.71	107.57	0.43	0.50	95.15	108.07
11.0	92.22	104.58	0.28	0.32	92.50	104.90
11.5	89.36	101.20	0.00	0.00	89.36	101.20
12.0	86.42	97.77	0.00	0.00	86.42	97.77
12.5	83.61	94.49	0.00	0.00	83.61	94.49
13.0	81.04	91.48	0.00	0.00	81.04	91.48
13.5	78.13	88.11	0.00	0.00	78.13	88.11
14.0	75.24	84.79	0.00	0.00	75.24	84.79
14.5	72.37	81.49	0.00	0.00	72.37	81.49
15.0	69.61	78.33	0.00	0.00	69.61	78.33
15.5	66.65	74.95	0.00	0.00	66.65	74.95
16.0	63.69	71.59	0.00	0.00	63.69	71.59
16.5	60.70	68.20	0.00	0.00	60.70	68.20
17.0	57.79	64.89	0.00	0.00	57.79	64.89
17.5	54.76	61.46	0.00	0.00	54.76	61.46
18.0	51.71	58.01	0.00	0.00	51.71	58.01
18.5	48.79	54.72	0.00	0.00	48.79	54.72
19.0	46.21	51.80	0.00	0.00	46.21	51.80
19.5	43.56	48.80	0.00	0.00	43.56	48.80
20.0	41.52	46.50	0.00	0.00	41.52	46.50

### 3.2.2. Topographic data preparation in ArcGIS

The applicability of ArcGIS in watershed modelling has increased as a result of the availability of spatial information along with fast processors and user-friendly interfaces like RAS Mapper, HEC-GeoHMS, HEC-GeoRAS and Arc-Hydro. These linked hydraulic and hydrological models to the ArcGIS environment.

In our study, ArcMap was used to create DEM of the study area. Two sources of data were used to create the DEM. The first source was point data extracted as shape files from AutoCAD files obtained from BUSKI report (2013). The projection system used to extract point data from CAD files was European Datum 50/Transverse Mercator 30 (ED 50/TM 30). The second source was the scanned topographic maps with contour lines, also obtained from BUSKI. The projection system used for importing the scanned maps to ArcMap was European Datum 1950 UTM Zone 36N. A DEM with a resolution of 0.5 m for Ismetiye creek and its catchment area was obtained in Arc-Map. This DEM was then transferred as a terrain to RAS Mapper window of HEC-RAS for modelling of the creek. In RAS Mapper, it was made sure that the DEM imported from ArcMap was georeferenced. This was checked by adding the google satellite view on the background of RAS Mapper interface.

#### A. Modelling for natural channel

1. The CAD files were set to appropriate coordinate system mentioned above and then imported to ArcMap. Figure 3.7 shows ArcMap interface after the CAD files were imported. There was a set of points with no elevation data assigned to them. These points were removed.

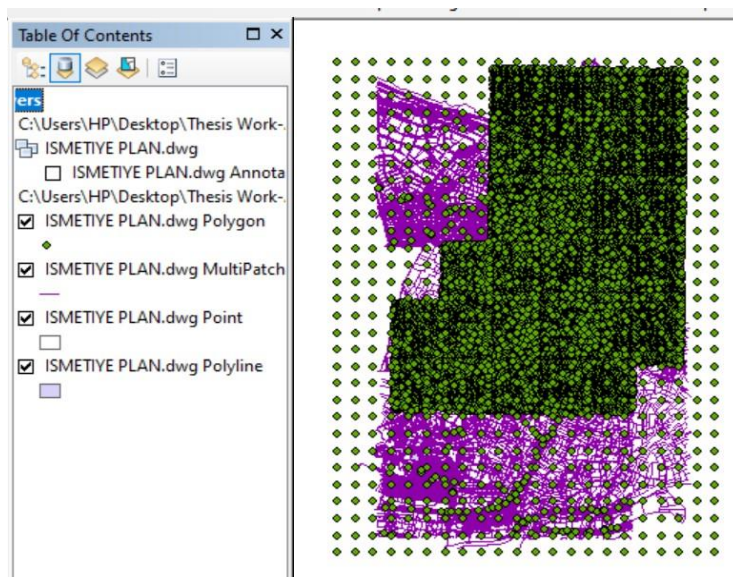


**Figure 3.7.** Shows the CAD data as it is imported to ArcMap

As shown in Figure 3.8, the point layer containing elevation data was converted to point shapefile in ArcMap.

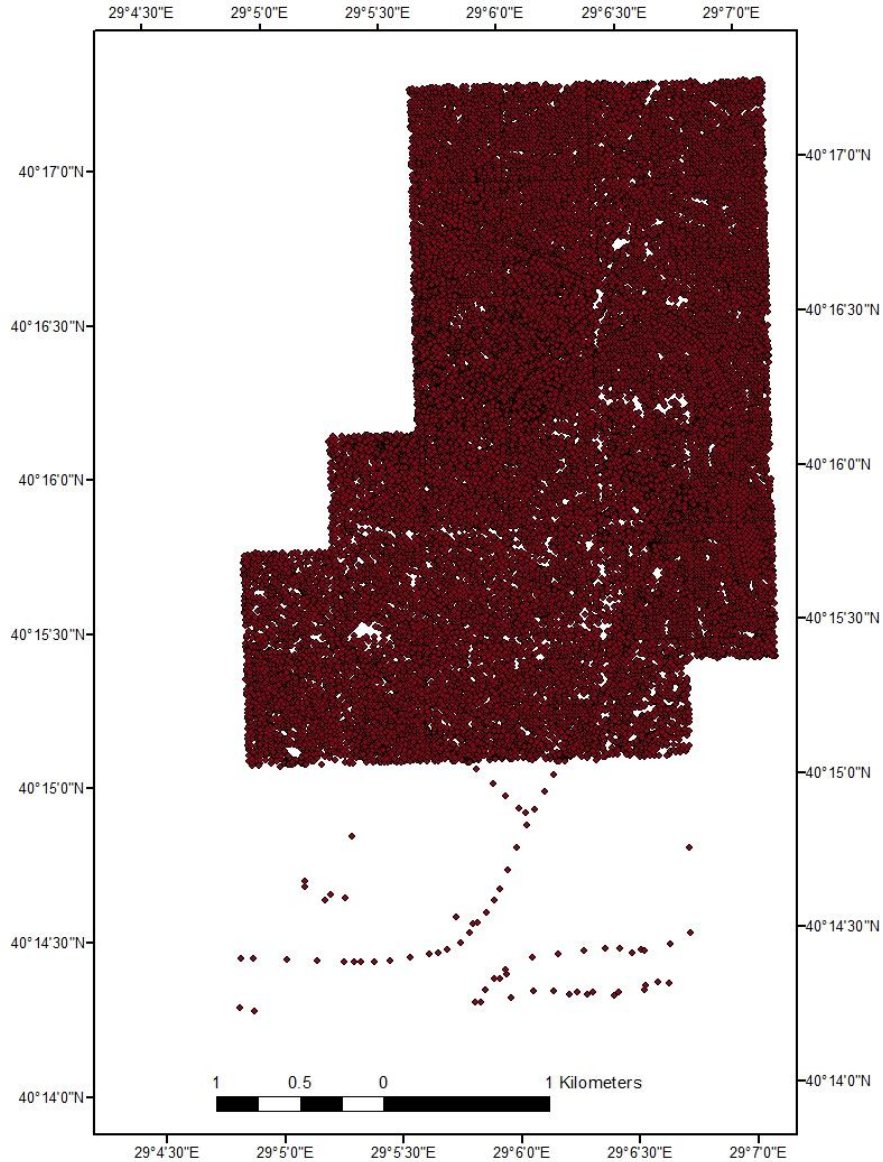


**Figure 3.8.** Point elevation data of Ismetiye channel and surrounding areas

As can be seen from Figure 3.8, there was scarce data available towards the downstream end of the channel. By using slope of the natural channel (0.006), further elevation data was added along the channel path until the end of Ismetiye creek. In addition to this, more elevation data was obtained from the second source consisting of scanned maps of study area. Points were drawn over contour

lines of the map and elevation corresponding to the contour line was assigned to them.

Thus, elevation data along the complete path of Ismetiye creek was obtained. This enabled us to model the complete channel until its confluence with Nilufer river. Figure 3.9 shows point elevation data of Ismetiye channel in its natural state after inserting additional elevation data.

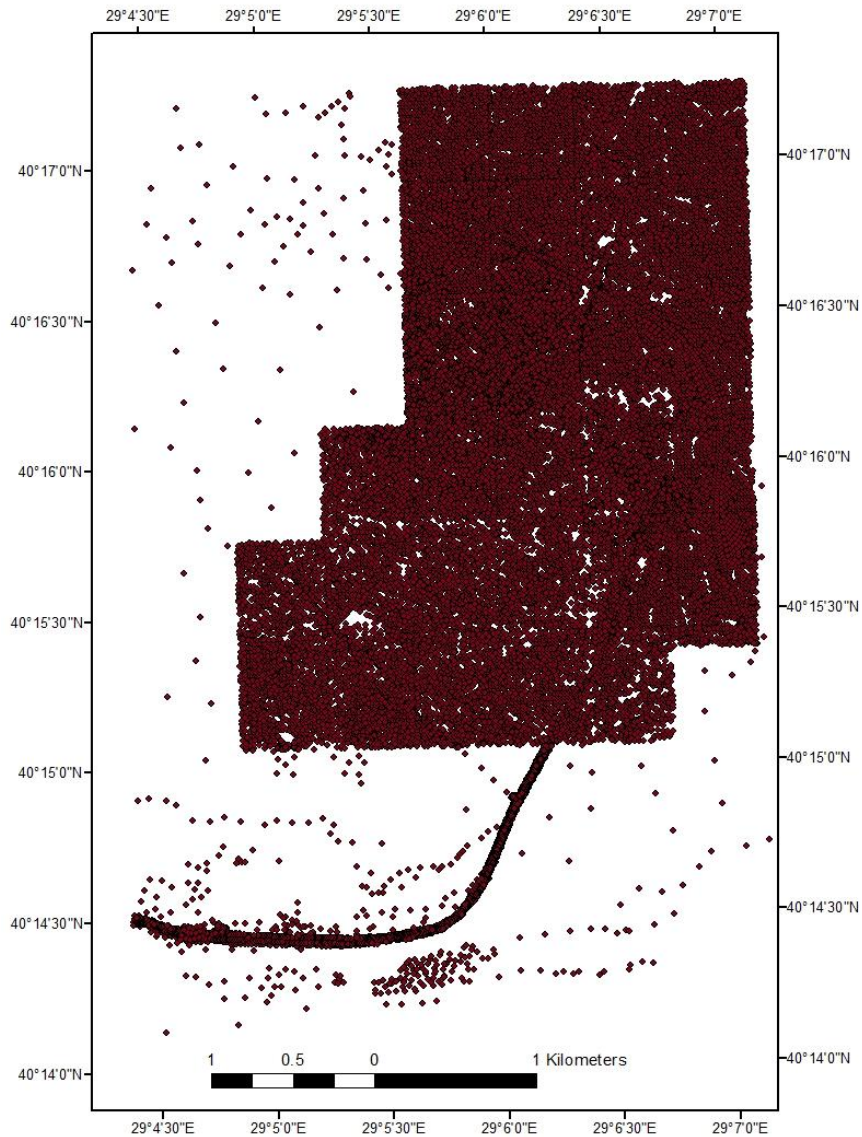


**Figure 3.9.** Point elevation data of Ismetiye channel and surrounding areas after inserting additional points in ArcMap.

- Using Inverse Distance Weighted (IDW) raster interpolation method, a DEM was created from the above point data. The cell size used for creating DEM in this study was 0.5m. The DEM is shown in Figure 3.10.

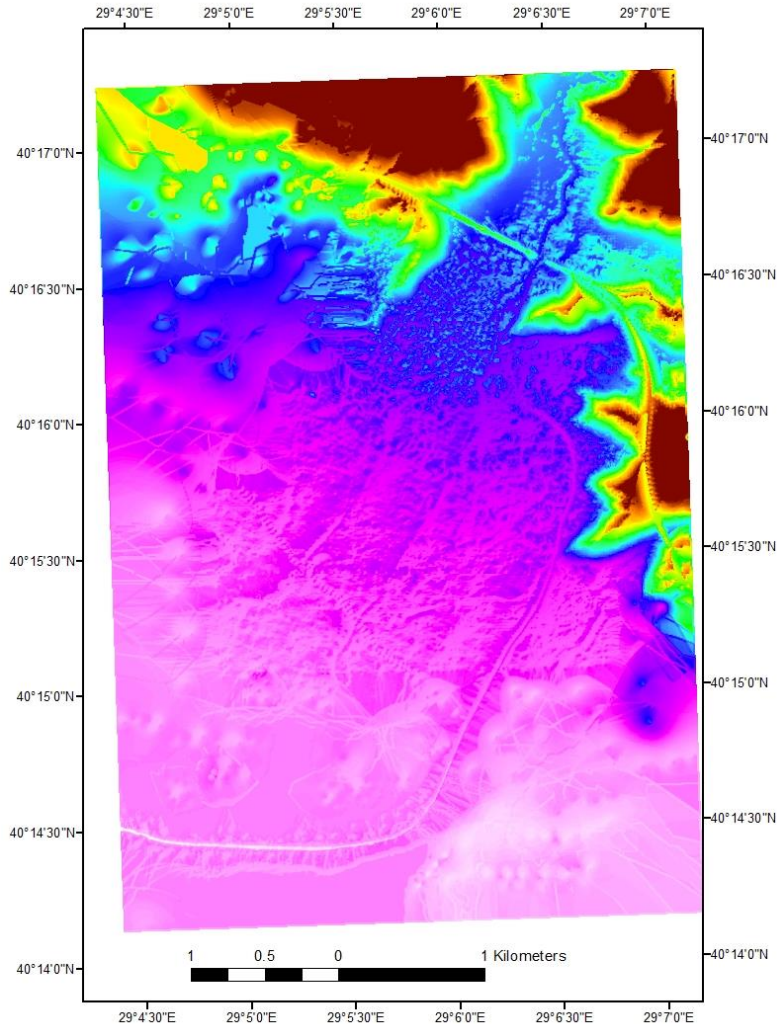


**Figure 3.10** DEM of resolution 0.5m as obtained from IDW raster interpolation method in Arc Map

DEM was exported to RAS Mapper by adding it in the terrain layer of RAS Mapper.

## **B. Modelling for concrete channel**

- Intermediate sections were inserted for the concrete channel.

Elevation data within the concrete channel was provided in the BUSKI report (2013). This data was available with a 20-m interval for a span of 4020 m. Slope of the concrete channel was 0.008484. For the remaining downstream part of channel, assuming the same slope of the channel throughout, intermediate sections were inserted at 20-m intervals by interpolation. This was done to obtain a DEM throughout the Ismetiye channel so as to run the simulation along the path of the entire channel. Figure 3.11 shows the intermediate sections inserted in the concrete channel.

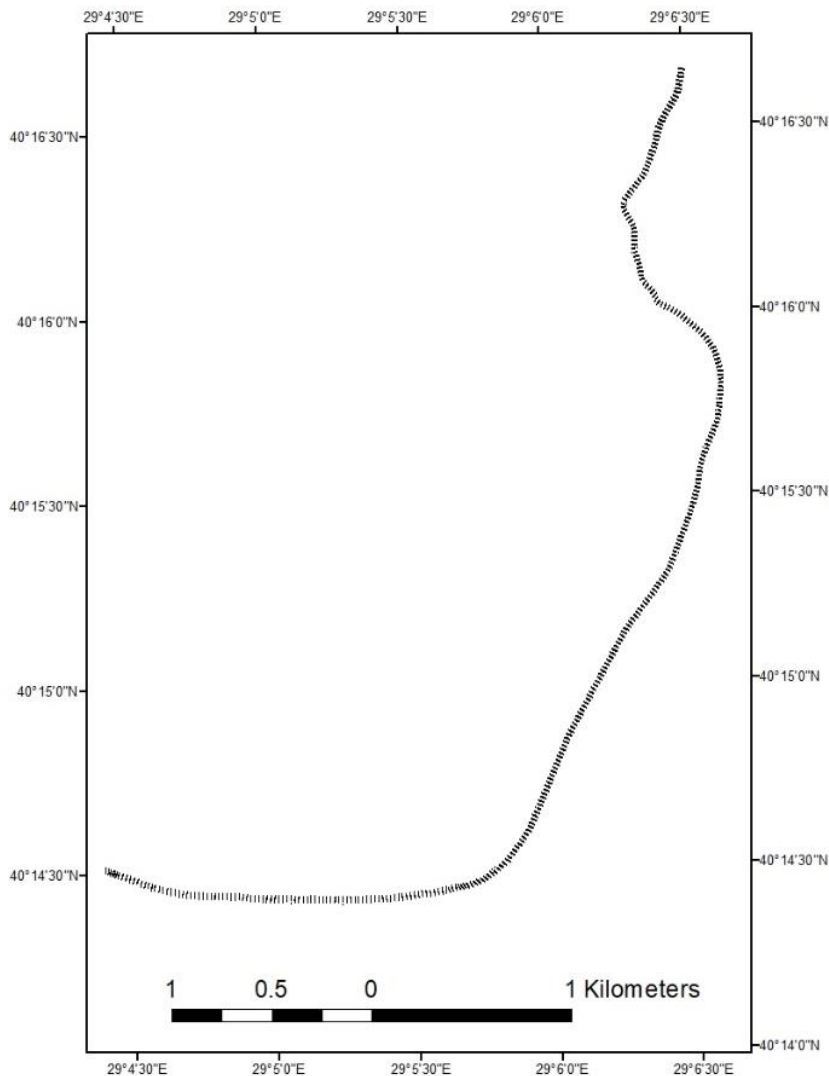


**Figure 3.11.** Intermediate sections in the concrete channel with 20-m intervals.

To obtain the DEM of the rehabilitated channel, the elevation data of natural channel was replaced by the elevation data of concrete channel. This was done by replacing the elevation data along the channel path by the intermediate sections as shown in the Figure 3.11 above. Figure 3.12 shows the point elevation data of Ismetiye channel in its rehabilitated state.

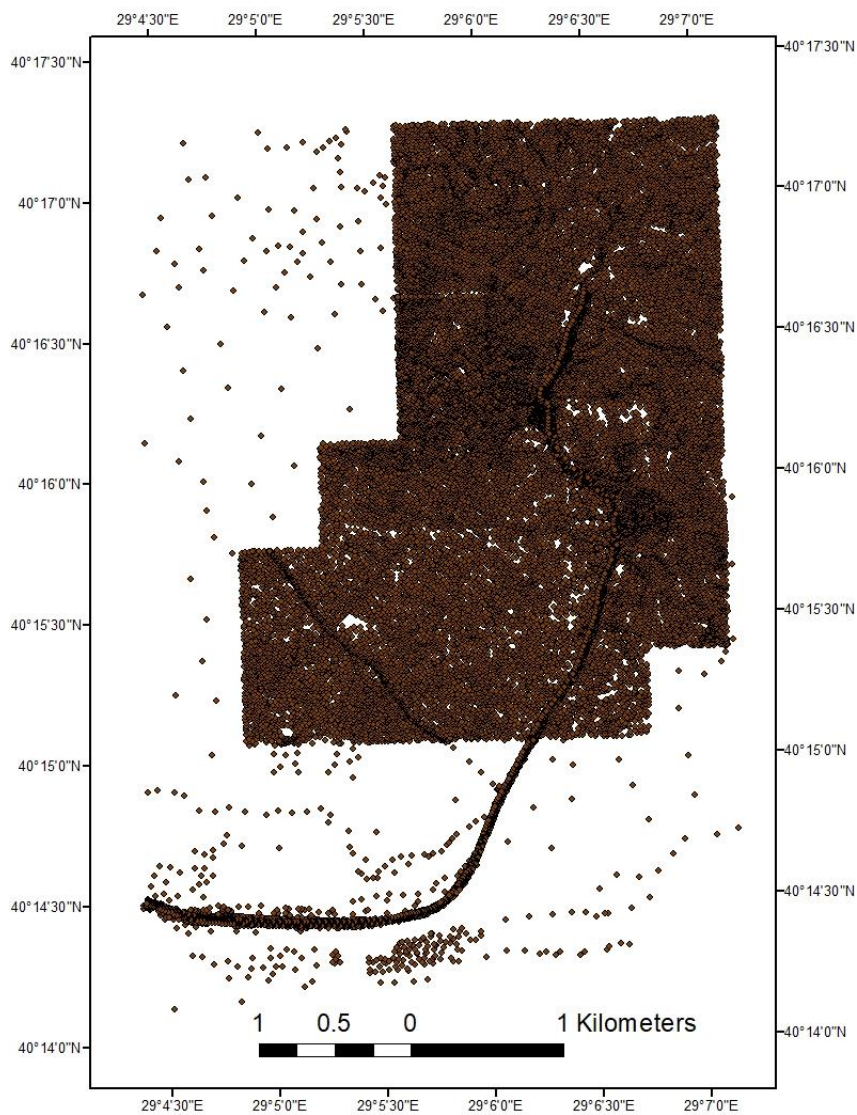


**Figure 3.12.** Point elevation data with concrete channel

- Using Inverse Distance Weighted (IDW) raster interpolation method, a DEM with a resolution of 0.5 m was created from the above point data. Figure 3.13 shows the DEM of the rehabilitated channel.

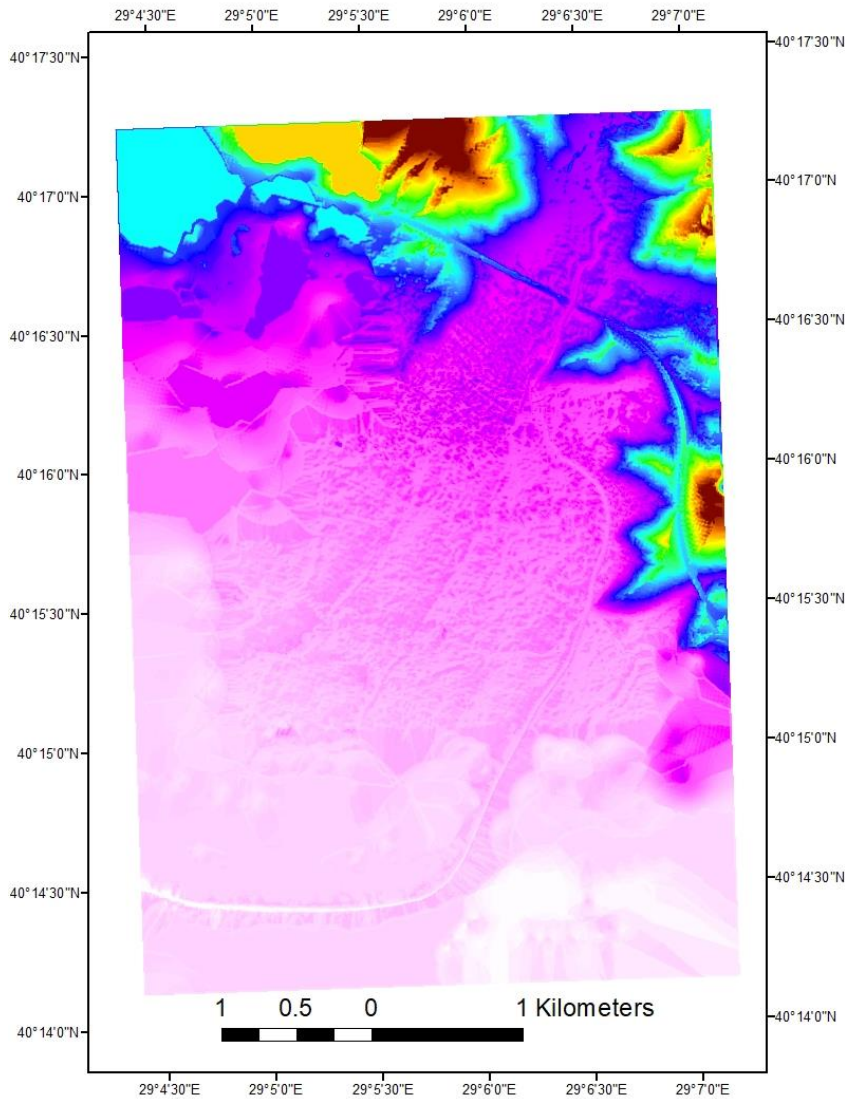


**Figure 3.13.** DEM of the rehabilitated channel

- DEM was exported to RAS Mapper by adding it in the terrain layer of RAS Mapper.

### 3.2.3. HEC-RAS

The abbreviation for HEC-RAS is the Hydrologic Engineering Centre's River Analysis System. As a hydraulic simulation model, it is used for calculating water surface profiles in both of man-made and natural channels. There are both 1-D and 2-D steady and unsteady simulation options. Additionally, there are also components for water quality analysis and sediment transport.

Steady flow analysis is used to calculate water surface profiles for steady and gradually varied flows. Subcritical, supercritical and mixed flow regime water surface profiles can be modelled. It is also used to model hydraulic structures such as bridges, weirs and spillways. This software is widely used for flood insurance studies and for floodplain mapping and channel management owing to its wide modelling capabilities. An iterative procedure, which is used to solve energy equation, helps in the calculation of water surface profiles. For calculating rapidly varied profile, a momentum equation is used.

Following are the input requirements for a 1D-model:

- right and left channel bank locations
- channel and overbank elevations
- contraction and expansion coefficients
- Manning's roughness coefficients for channel and overbanks
- downstream cross-section distances
- flow data and
- boundary condition such as known water surface elevation, critical depth, normal depth, or rating curve

For one-dimensional simulations, HEC-RAS is using 1D Saint Venant equation. Energy and momentum equations are used to derive 1D Saint Venant equation which in turn solves steady-state and unsteady-state flow water surface profile simulation in HEC-RAS. In HEC-RAS, the unsteady flow simulation component can simulate 1D unsteady flow through a full network of open channels. Implicit finite difference method is used. The

continuity and momentum equations are shown as Eq. (3.1) and Eq. (3.2) (HEC-RAS User's Manual 2020).

$$\frac{\delta A}{\delta t} + \frac{\delta Q}{\delta x} - q = 0 \quad (3.1)$$

$$\frac{\delta Q}{\delta t} + \frac{\delta(VQ)}{\delta x} + gA \left( \frac{\delta z}{\delta x} + S_f \right) = 0 \quad (3.2)$$

Here,  $A$  is the cross-sectional area,  $t$  is the time,  $Q$  is the discharge,  $q$  is the inflow per unit area,  $x$  is the distance along the channel,  $V$  is the velocity,  $z$  is the elevation,  $S_f$  is the friction slope and,  $g$  is the gravitational acceleration.

With the help of RAS Mapper version, the dependency on ArcGIS for flood mapping was eliminated.

#### **3.2.4. 2D-modelling in HEC-RAS**

The terrain files of the study area obtained for both before and after the rehabilitation of Ismetiye creek were used in HEC-RAS 6.0 Beta Version to run 2D simulations. Discharge values with 500-year and 1000-year return periods,  $Q_{500}$  and  $Q_{1000}$ , for a 20-hour hydrograph were used as inflow boundary conditions.

The HEC-RAS two-dimensional computational module has the option of running the following equation sets: 2D Diffusion Wave equations; Shallow Water Equations (SWE-ELM) with a Eulerian-Lagrangian approach to solving for advection; or a new Shallow Water Equation solver (SWE-EM) that uses a Eulerian approach for advection. The new SWE solution method is more momentum conservative but may require smaller time steps and produce longer run times. The default is the 2D Diffusion Wave equation set. In general, many flood applications work fine with the 2D Diffusion Wave equations. The Diffusion Wave equation set runs faster and is inherently more stable. However, there are applications where the 2D SWE should be used for greater accuracy. The 2D

Diffusion Wave computational method is the default solver. Most 2D modeling situations, such as flood modelling, can be accurately modeled using this solver, where inertial forces tend to dominate frictional and other forces (HEC-RAS User's Manual 2020).

The Diffusion Wave computational method can be used in the following situations:

- Flow is mainly driven by gravity and friction
- Fluid acceleration is monotonic and smooth (i.e., no waves)
- Compute rough global estimates (i.e., flood extents)
- Assess interior flooding (i.e., levee breach)
- Quick estimate for using the Full Momentum computational method

The following guidelines as shown in Eq. (3.3) and Eq. (3.4) are used for picking a computation interval for the Diffusion Wave Equations:

$$C = \frac{V\Delta T}{\Delta x} \leq 2.0 \quad (3.3)$$

For  $C = 2.0$

$$\Delta T \leq \frac{2\Delta x}{V} \quad (3.4)$$

Where  $C$  = Courant Number

$V$  = flood wave velocity m/s

$\Delta t$  = computational time step (s)

$\Delta x$  = average cell size (m)

Steps followed in HEC-RAS for 2D simulations:

1. Open the RAS Mapper menu of HEC-RAS. From 'Project' tab, add the relevant projection file by clicking on 'Set Projection' as shown in the Figure 3.14 below.

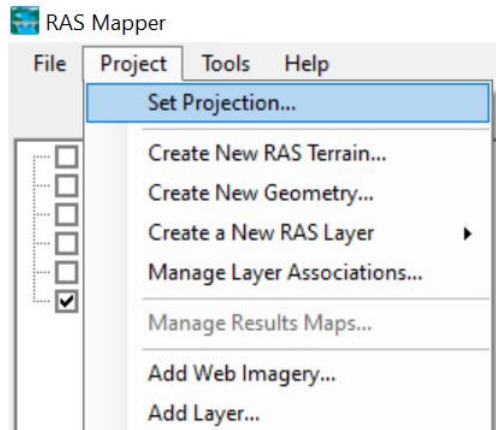


**Figure 3.14.** Setting projection to the RAS Mapper file.

2. Import the DEM created in ArcMap to RAS Mapper by right clicking on the 'Terrain' layer and selecting 'Create a New RAS Terrain' as shown in the Figure 3.15.

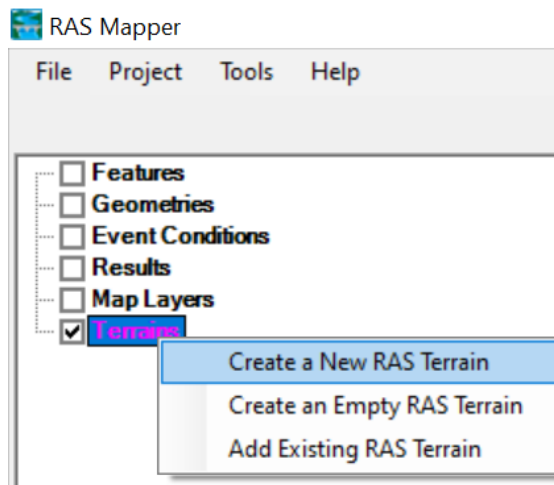


**Figure 3.15.** Adding terrain to the RAS Mapper file

- To do any modifications to the terrain such as adding buildings, bridges, roadways and channels, right click on the 'Terrain' layer and click on 'Add New Modification Layer', as shown in the Figure 3.16. Draw the buildings, bridges, roadways, channels and other structures present in the study area and assign relevant elevations to them to make the terrain look more realistic. The terrain before and after modifications are shown in the Figure 3.17.

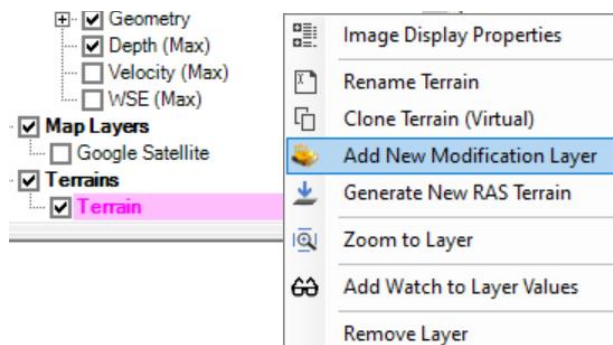


**Figure 3.16.** Adding a new modification layer to the RAS Mapper file

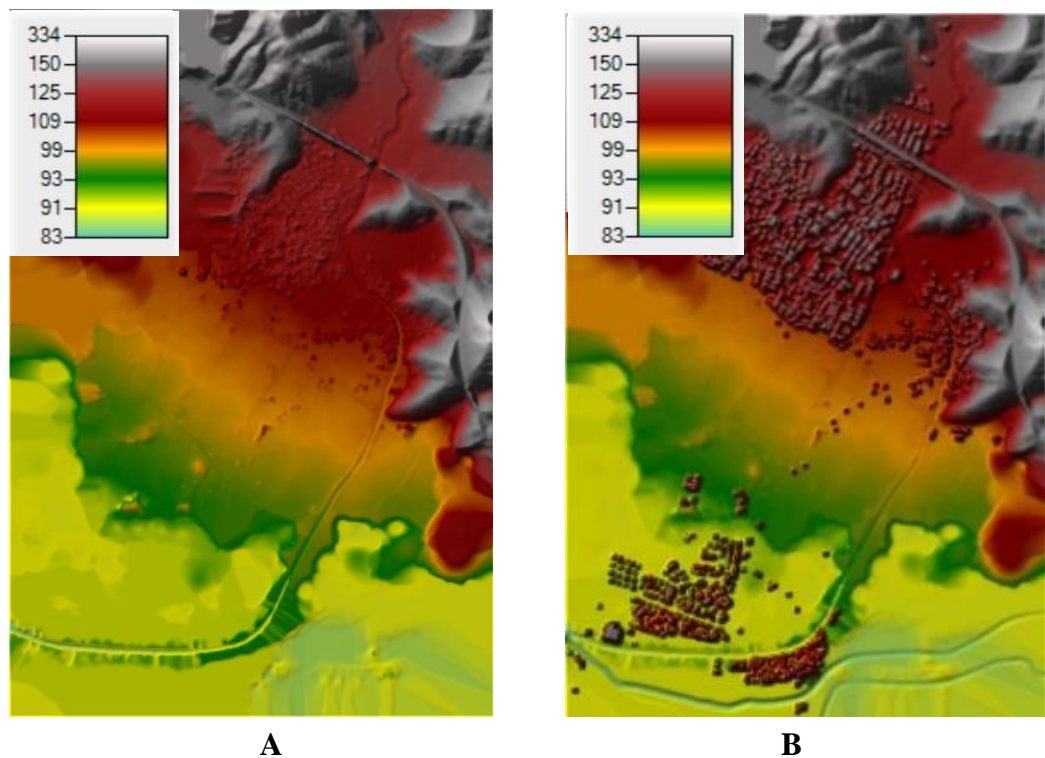


**Figure 3.17.** Terrain in RAS Mapper **A)** before modification **B)** after modification

- Flow area is defined over the entire terrain. In order to define a flow area, add a new geometry by right clicking on the 'Geometry' layer and selecting 'Add New Geometry' as shown in the Figure 3.18.

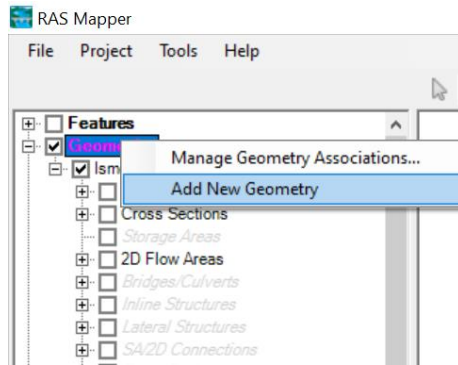


**Figure 3.18.** Adding geometry of the channel in RAS Mapper

In the layer 'Geometries', right click on '2D Flow Areas' and define the flow area by editing the geometry as shown in the Figure 3.19.

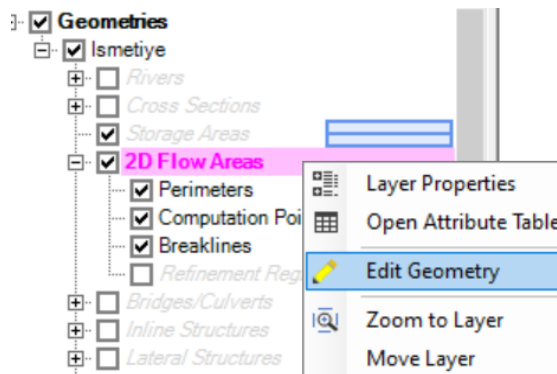


**Figure 3.19.** Editing geometry to define flow area in RAS Mapper

As shown in the Figure 3.20, right click on the layer 'Perimeter' and 'Edit 2D Area Properties' to define flow area and size of the mesh which was set as 10 m in our case. Figure 3.21 shows the flow area and the mesh size.

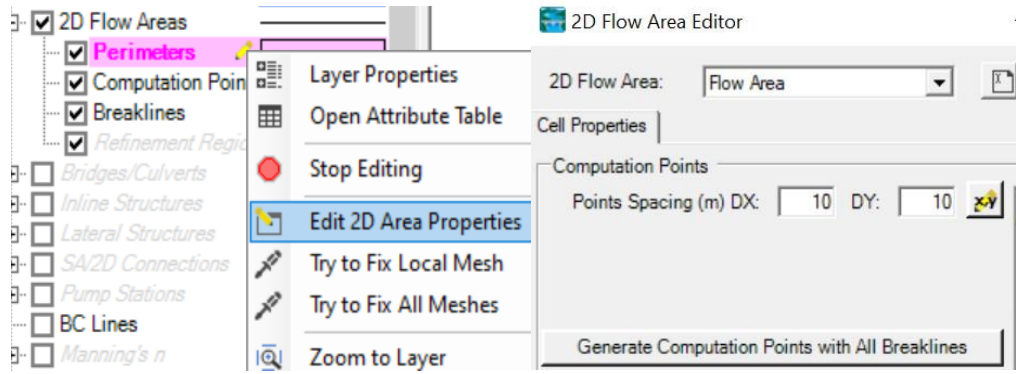


**Figure 3.20.** Defining the mesh size in RAS Mapper

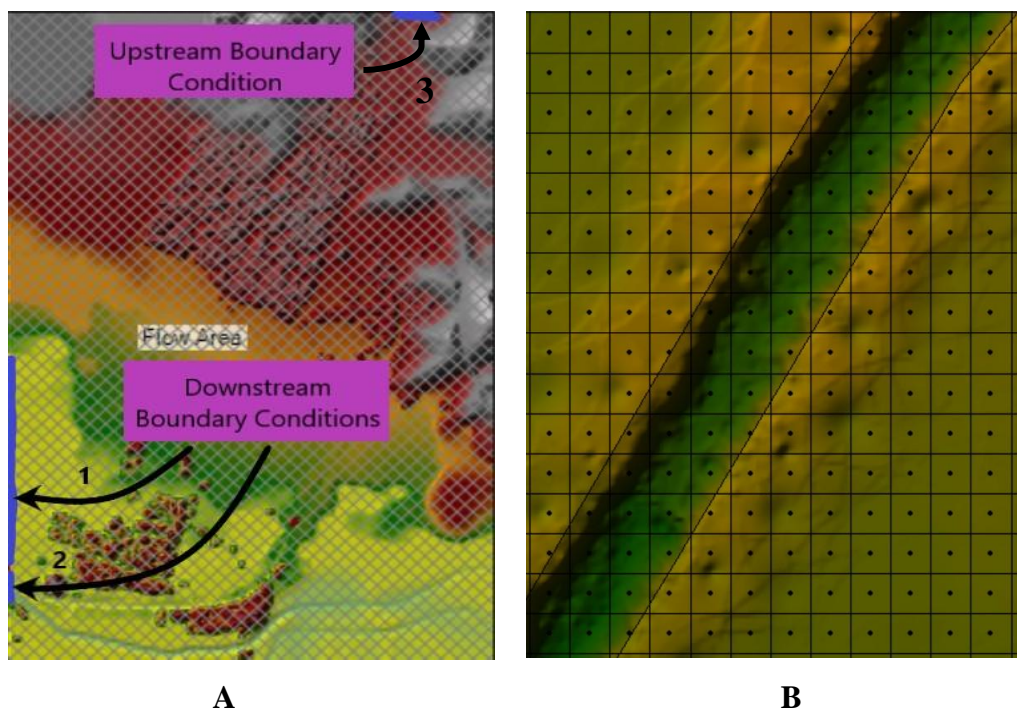


**Figure 3.21.** Flow area showing **A)** boundary conditions **B)** mesh size of 10 m

5. Under the layer '2D Flow Areas' right click on 'Breaklines' and then 'Edit Geometry', to readjust the mesh along the edges of the river by drawing lines along both edges of channel as shown in Fig 3.22.

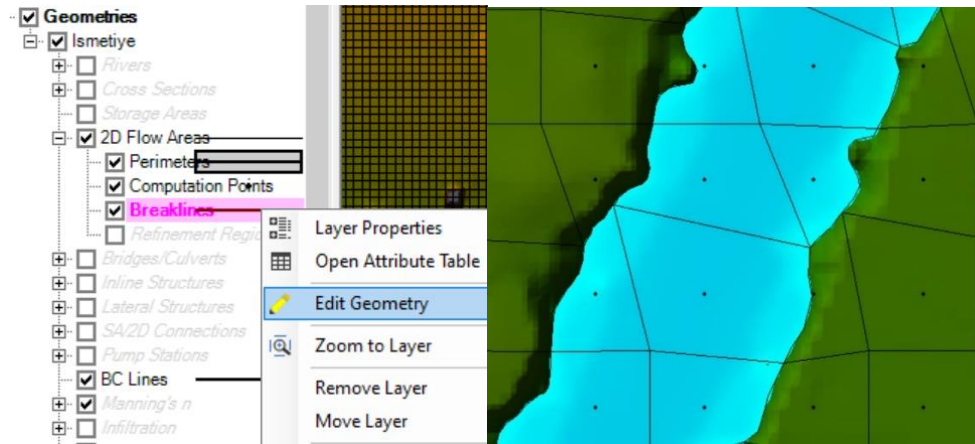


**Figure 3.22.** Refinement of 2D mesh in RAS Mapper by using ‘breaklines’

6. In order to specify the boundary conditions, under the layer ‘BC lines’, draw boundary lines at the upstream (1) and downstream (2) ends of the channel as shown in Figure 3.23. In our case, since water was accumulating towards the end of the channel rather than flowing out of the flow area, we introduced another downstream boundary condition (3) with a gentle slope of 0.001 to ensure flowing out of water from the catchment area. The values of boundary conditions are specified in step 9.

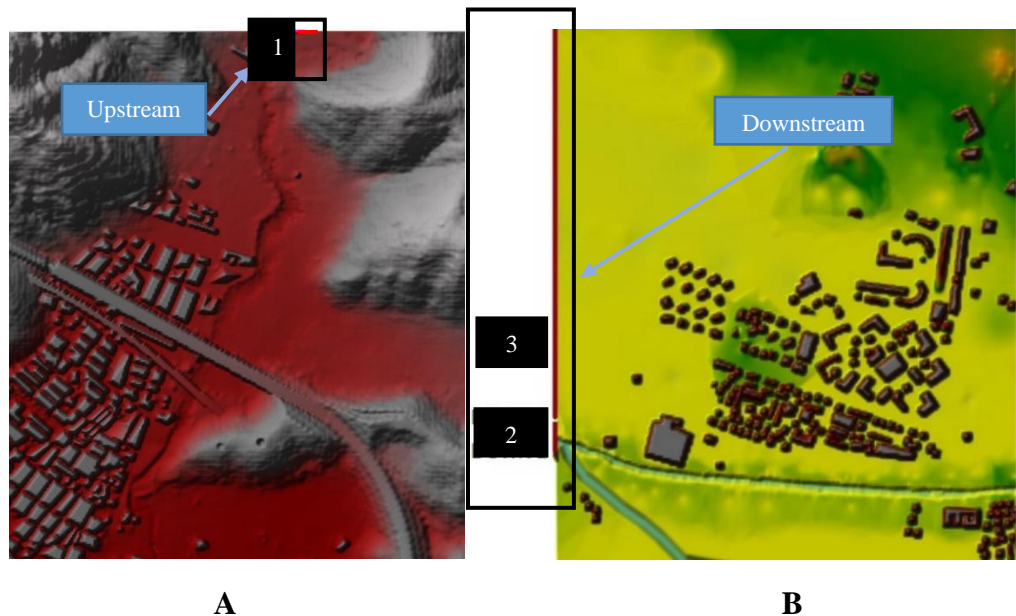


**Figure 3.23.** Magnified view of the terrain showing boundary lines on A) upstream end of the channel B) downstream end of the channel.

7. Assign Manning's n value to the channel by right clicking on 'Calibration Region' under 'Manning's n' layer and defining the channel geometry for which Manning's n value is to be assigned. The Manning's n value for natural channel was taken as 0.05 and for concrete channel, it was taken as 0.012 (Chow, 1959). In case of rehabilitated channel, main channel was assigned a Manning's n value of 0.012 and overbank regions were assigned a Manning's n value of 0.05. Figure 3.24 shows where to assign Manning's n value to the channel. Also, polygons drawn in case of rehabilitated channel are shown along with their Manning's n values.

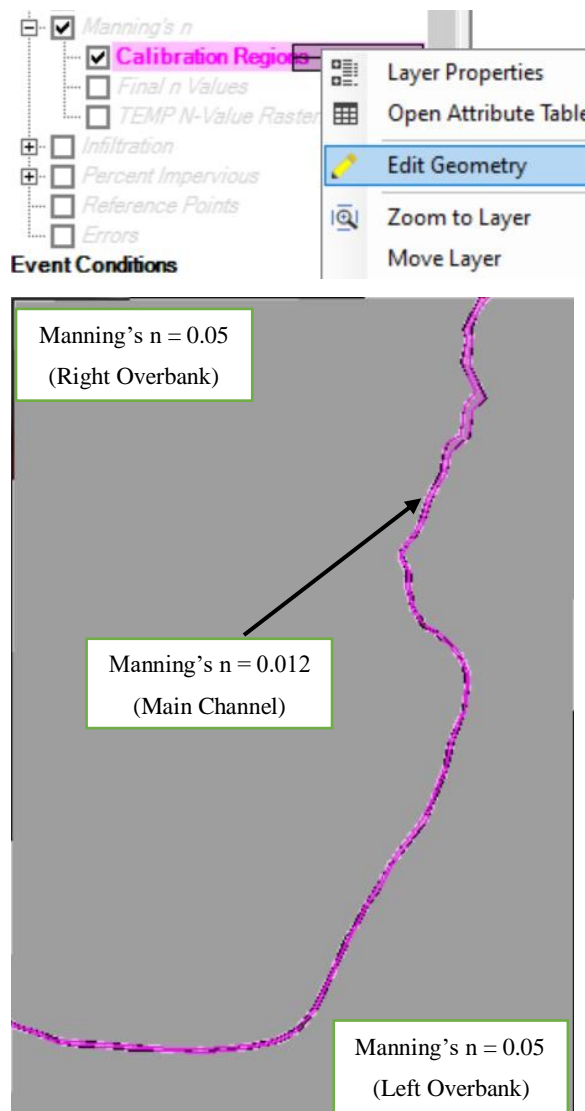


**Figure 3.24.** Assigning Manning's n value to the concrete channel and overbanks

- Save the file in Ras Mapper and import the geometry to 'view/edit geometry data' layer of HEC-RAS menu as shown in Figure 3.25.

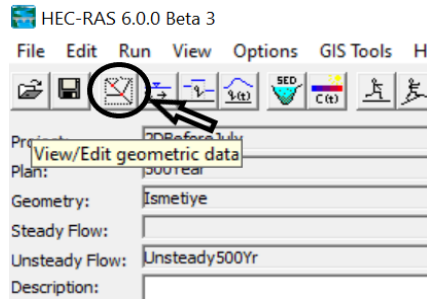


**Figure 3.25.** Importing the RAS Mapper file to HEC-RAS geometry

- In the 'view/edit unsteady flow data' section, add the boundary conditions; flow hydrograph for upstream (given in Table 3.2) and friction slope for downstream are specified as depicted in the Figure 3.26.

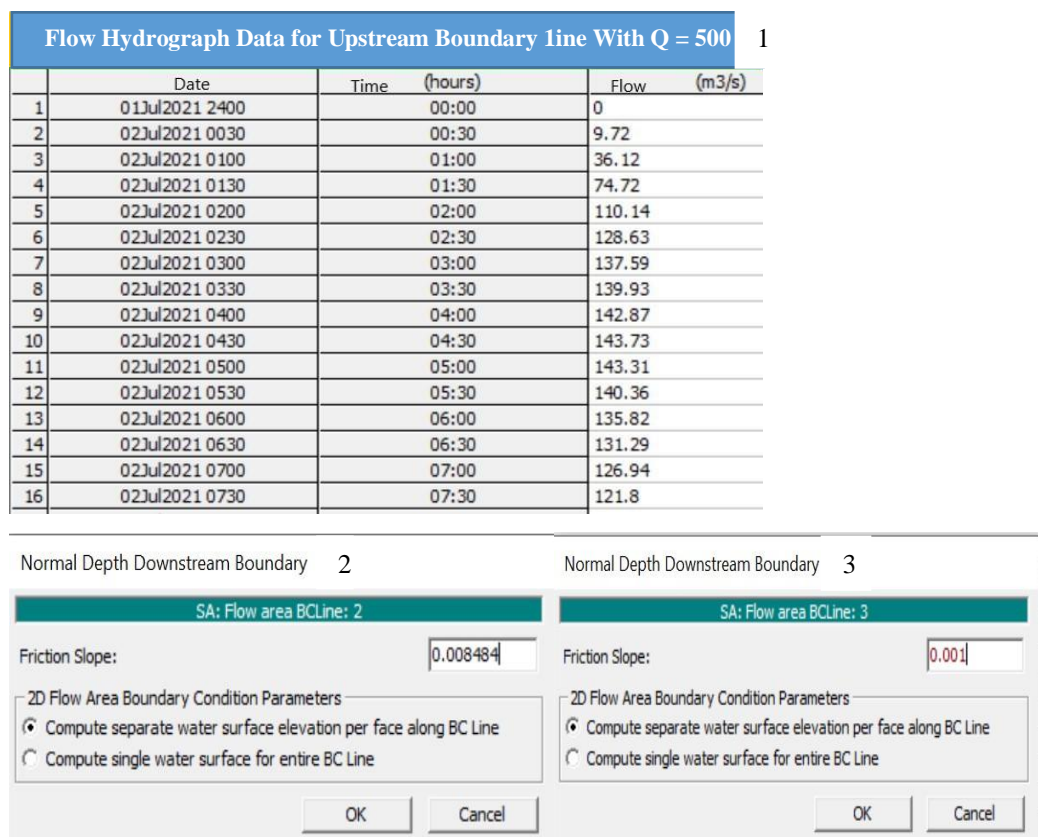


**Figure 3.26.** Adding flow hydrograph and friction slope to boundary conditions

10. Perform the unsteady flow simulation for a 20-hour hydrograph as shown in Figure 3.27.

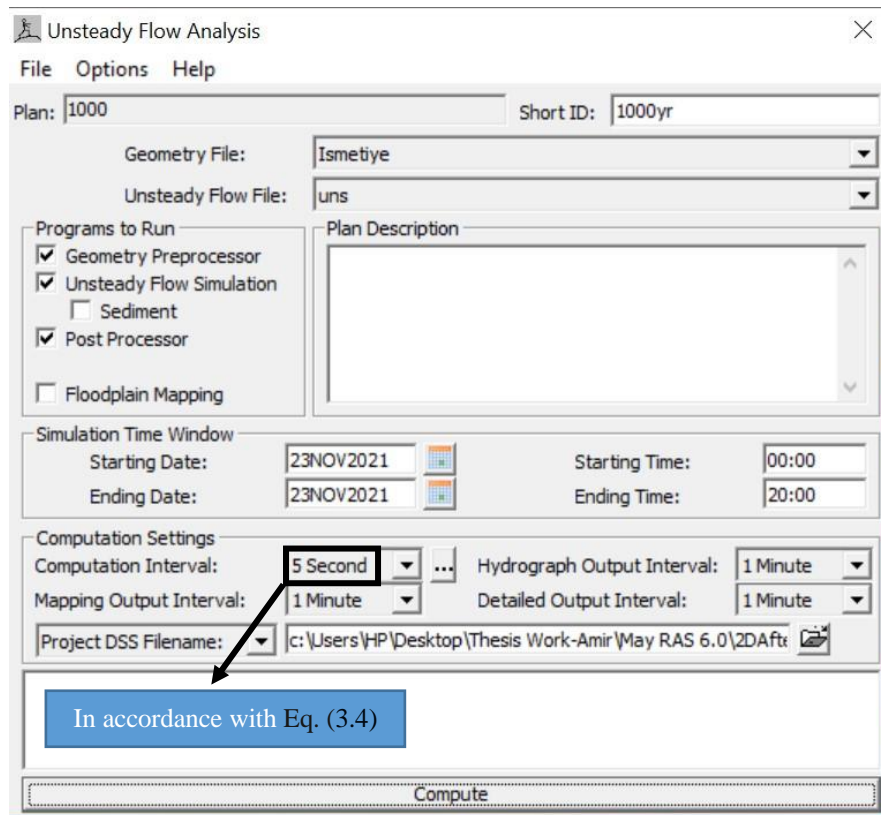


**Figure 3.27.** Performing unsteady flow simulation

Please note that the selection of  $\Delta x$  (average cell size) and  $\Delta t$  (computation interval) is a balance between achieving good numerical accuracy while minimizing computational time. In our study,  $\Delta x = 10$  metres and  $\Delta t = 5$  seconds, which was calculated from Eq. (3.4), achieved favourable results.

## 4. RESULTS AND DISCUSSION

In the simulations, discharge values with return periods of 500 and 1000 years ( $Q_{500}$  and  $Q_{1000}$ ) for a 20-hour hydrograph were used. The following 4 cases were modelled:

Case 1: Before rehabilitation of Ismetiye creek with  $Q_{500}$ .

Case 2: Before rehabilitation of Ismetiye creek with  $Q_{1000}$ .

Case 3: After rehabilitation of Ismetiye creek with  $Q_{500}$ .

Case 4: After rehabilitation of Ismetiye creek with  $Q_{1000}$ .

### 4.1. Results of 2D Simulation Before Rehabilitation of Ismetiye Creek

There was a significant flooding throughout the catchment area of Ismetiye creek as shown in Figure 4.1 and Figure 4.2. In the case of  $Q_{500}$ , the time of maximum extent is 7 hours 12 minutes and the maximum depth is 5.0 m as shown in Figure 4.1.

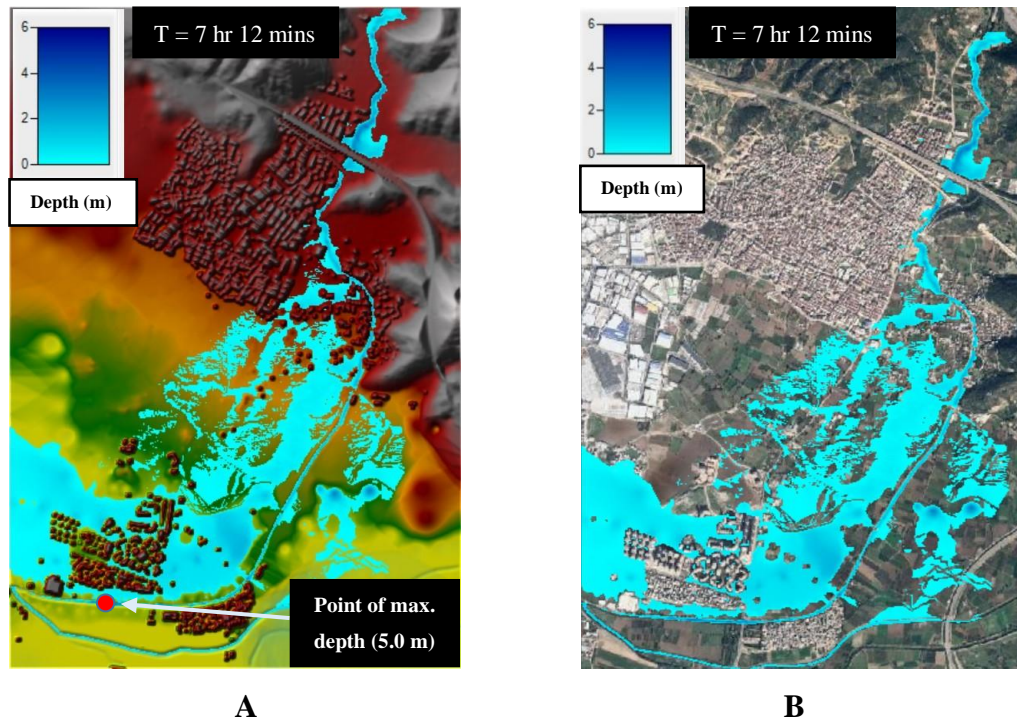


**Figure 4.1.** Case 1: Flood map for  $Q_{500}$  before rehabilitation A) HEC-RAS terrain view B) Google satellite view

For  $Q_{1000}$ , the time of maximum extent for is 7 hour 12 minutes and the maximum depth is 5.12 m.

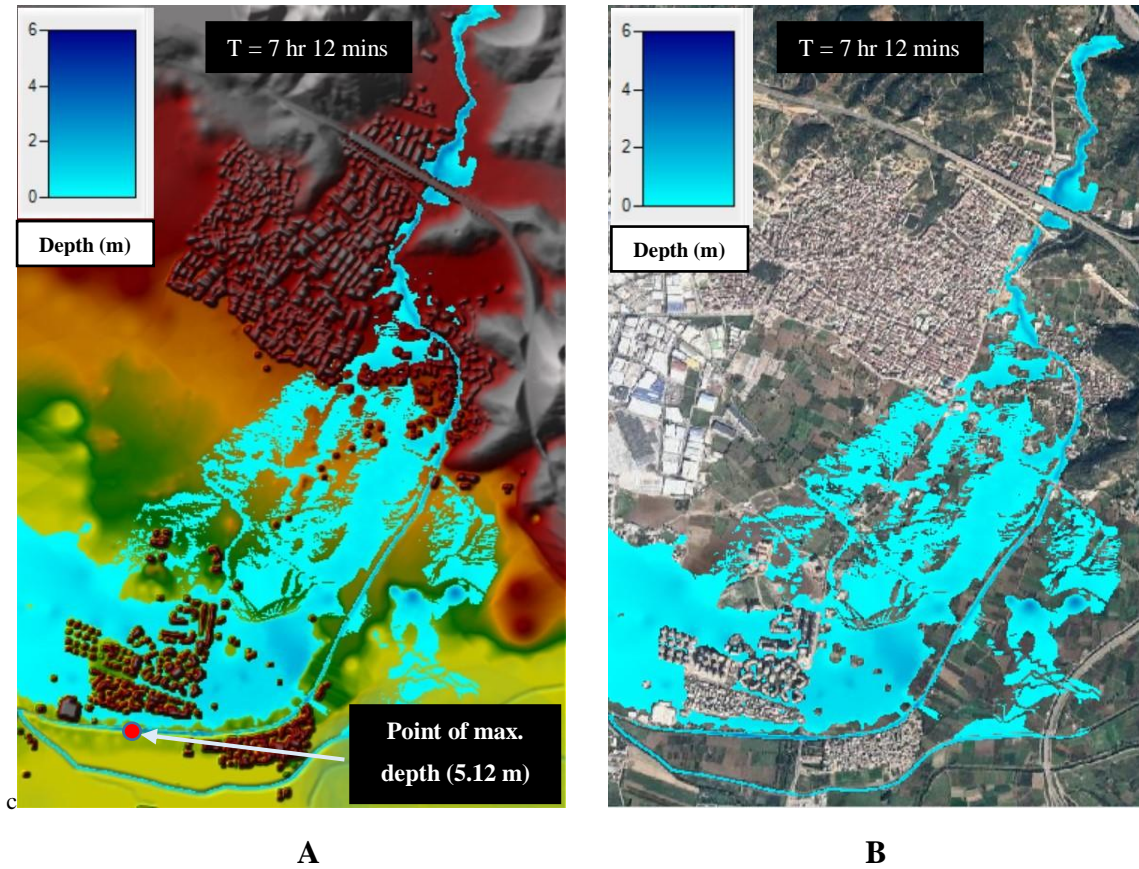


**Figure 4.2.** Case 2: Flood map for  $Q_{1000}$  before rehabilitation A) HEC-RAS terrain view B) Google satellite view

#### 4.2. Results of 2D Simulation After Rehabilitation of Ismetiye Creek

In the case of simulation after rehabilitation of Ismetiye Creek, it was found that flooding decreased significantly as compared to the case of natural channel. Figure 4.3 and Figure 4.4 show the flood maps after rehabilitation for  $Q_{500}$  and  $Q_{1000}$  respectively. For  $Q_{500}$ , the time of maximum extent is 7 hour 52 minutes and the maximum depth is 5.544 m. For  $Q_{1000}$ , the time of maximum extent is 7 hour 52 minutes and the maximum depth is 5.794 m.

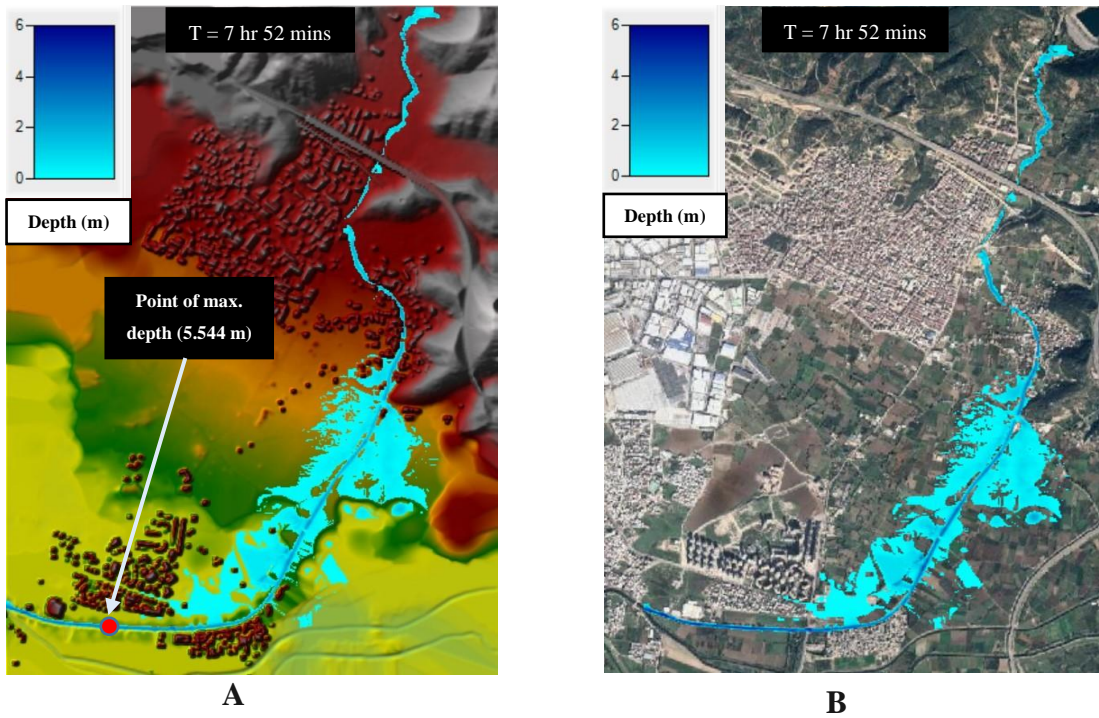


**Figure 4.3.** Case 3: Flood map for  $Q_{500}$  after rehabilitation A) HEC-RAS terrain view B) Google satellite view

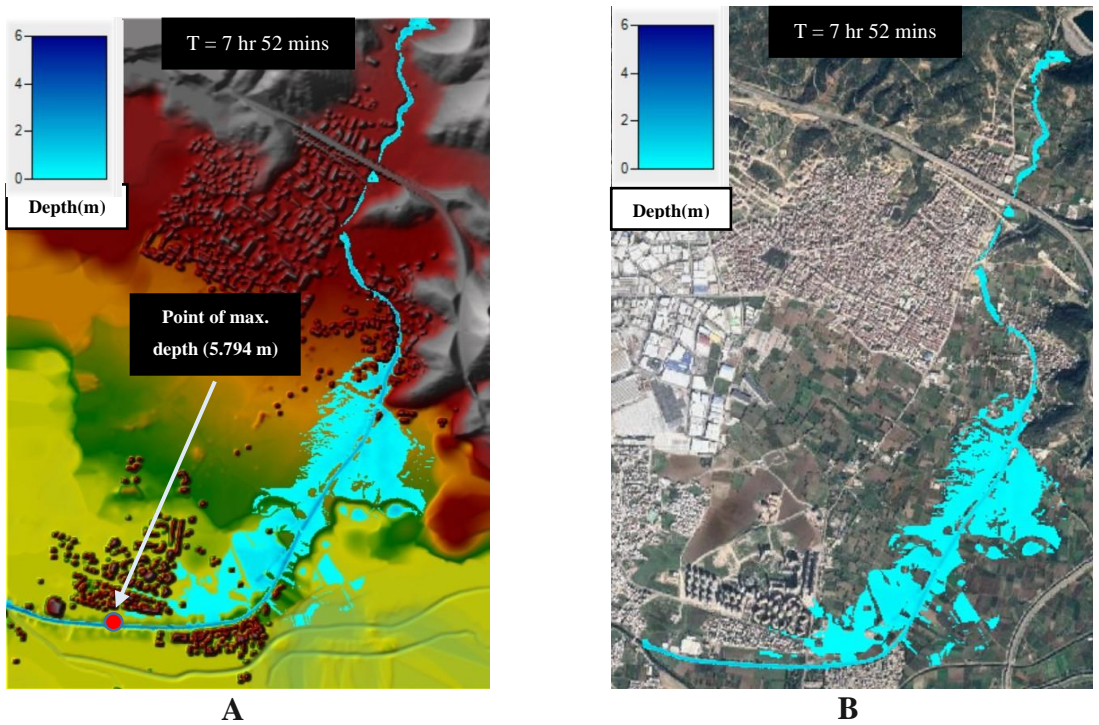


**Figure 4.4.** Case 4: Flood map for  $Q_{1000}$  after rehabilitation A) HEC-RAS terrain view B) Google satellite view

### 4.3. Comparison of results before and after the rehabilitation of Ismetiye creek

Figure 4.5 shows the comparison of flooding before and after rehabilitation for  $Q_{500}$ .

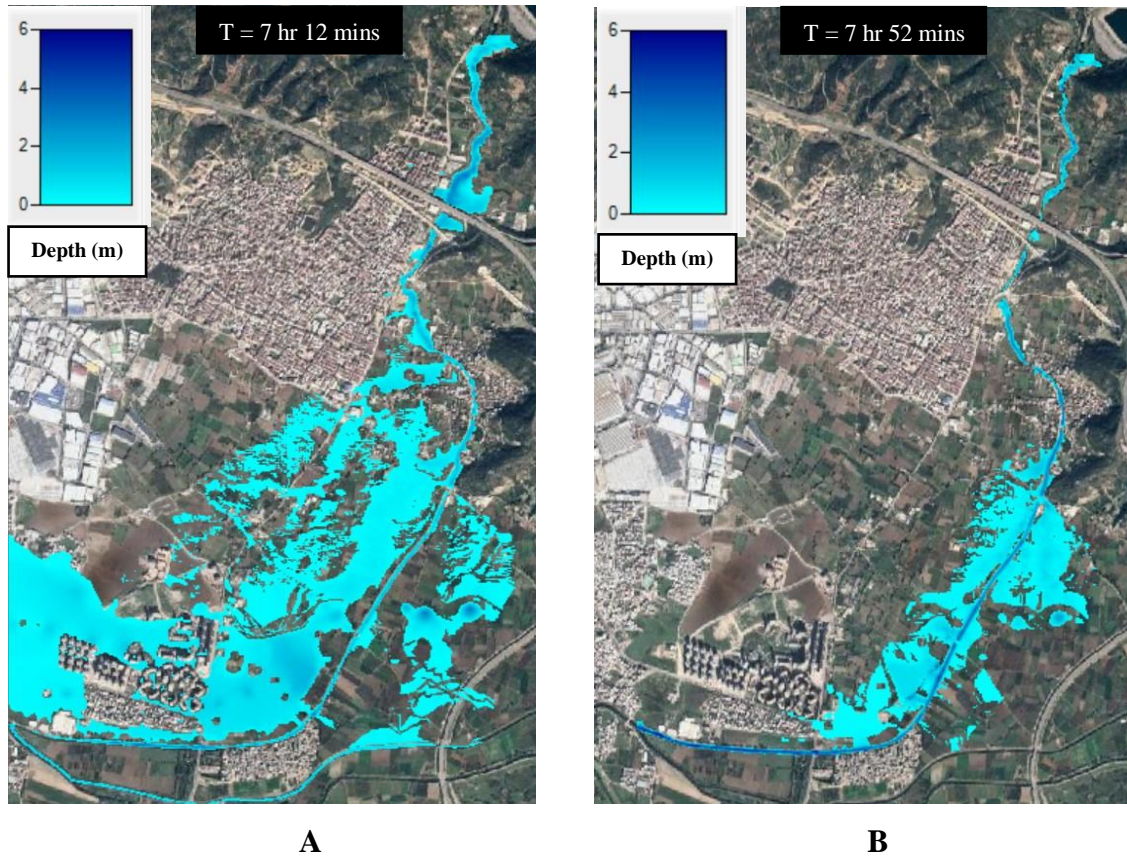


**Figure 4.5.** The comparison of flood maps for  $Q_{500}$  **A)** before rehabilitation **B)** after rehabilitation

Before rehabilitation, the extent of flooding was more at the beginning of the channel. As we go downstream, there was overbank flow observed which resulted in the flooding of catchment area. The overbank flow also flooded the dry channel present in the south of the Ismetiye creek. Moreover, new settlement region located on the right overbank side of downstream end of the channel also observed flooding.

On the other hand, after rehabilitation, there was more flow inside the main channel and less on the overbanks. The new settlements in the downstream were not inundated at all. Also, the channel in south of Ismetiye creek was not flooded at all.

Figure 4.6 shows the comparison of flooding before and after rehabilitation for  $Q_{1000}$ .

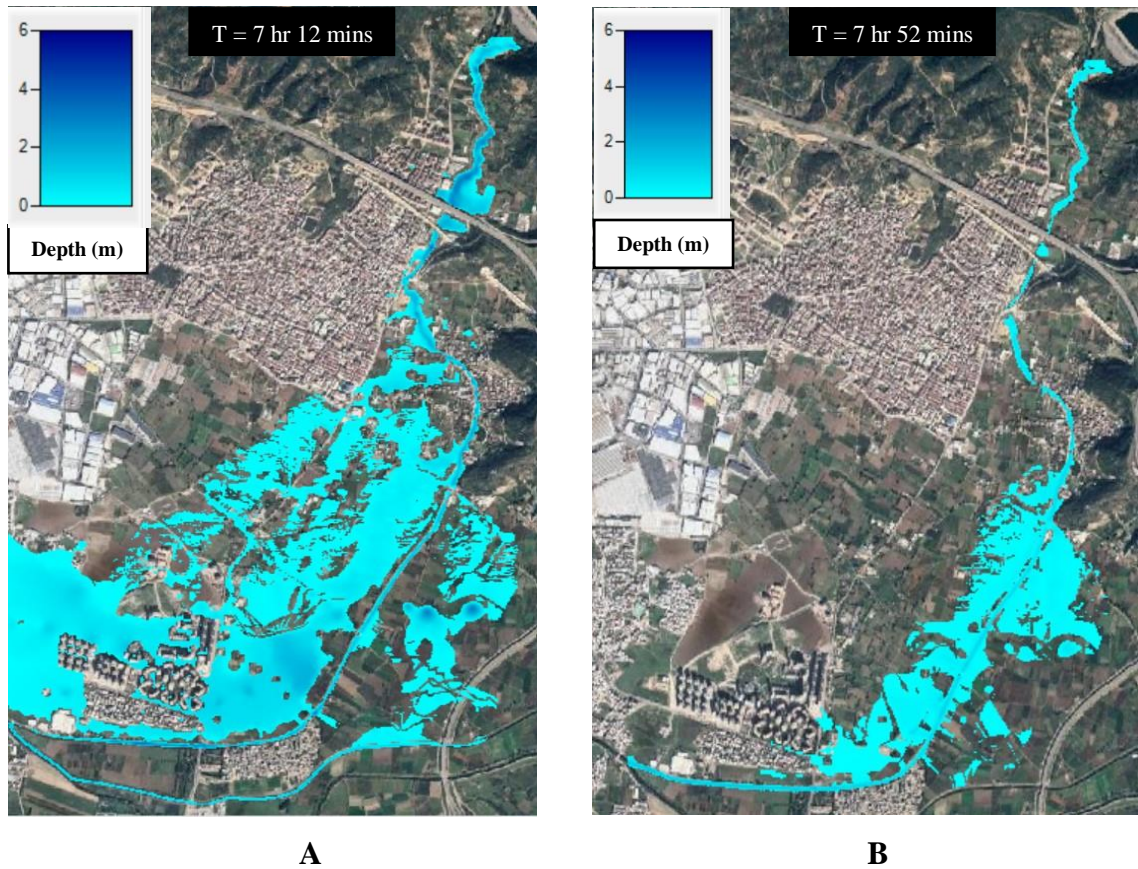


**Figure 4.6.** The comparison of flood maps for  $Q_{1000}$  **A)** before rehabilitation **B)** after rehabilitation

As expected, the extent of flooding observed for  $Q_{1000}$  was more than that of  $Q_{500}$ . The maximum depth observed in case of  $Q_{1000}$  was also higher as compared to that of  $Q_{500}$ . Before rehabilitation, maximum depth for  $Q_{500}$  was 5.0 m while for  $Q_{1000}$ , it was 5.12 m. On the other hand, after rehabilitation, maximum depth in case of  $Q_{500}$  was 5.544 m while for  $Q_{1000}$ , it was 5.794 m. Clearly, the maximum depths were higher after rehabilitation because of the fact that more water was retained in the main channel.

Figure 4.7 shows the comparison of velocity maps for  $Q_{500}$  before and after rehabilitation of Ismetiye creek.

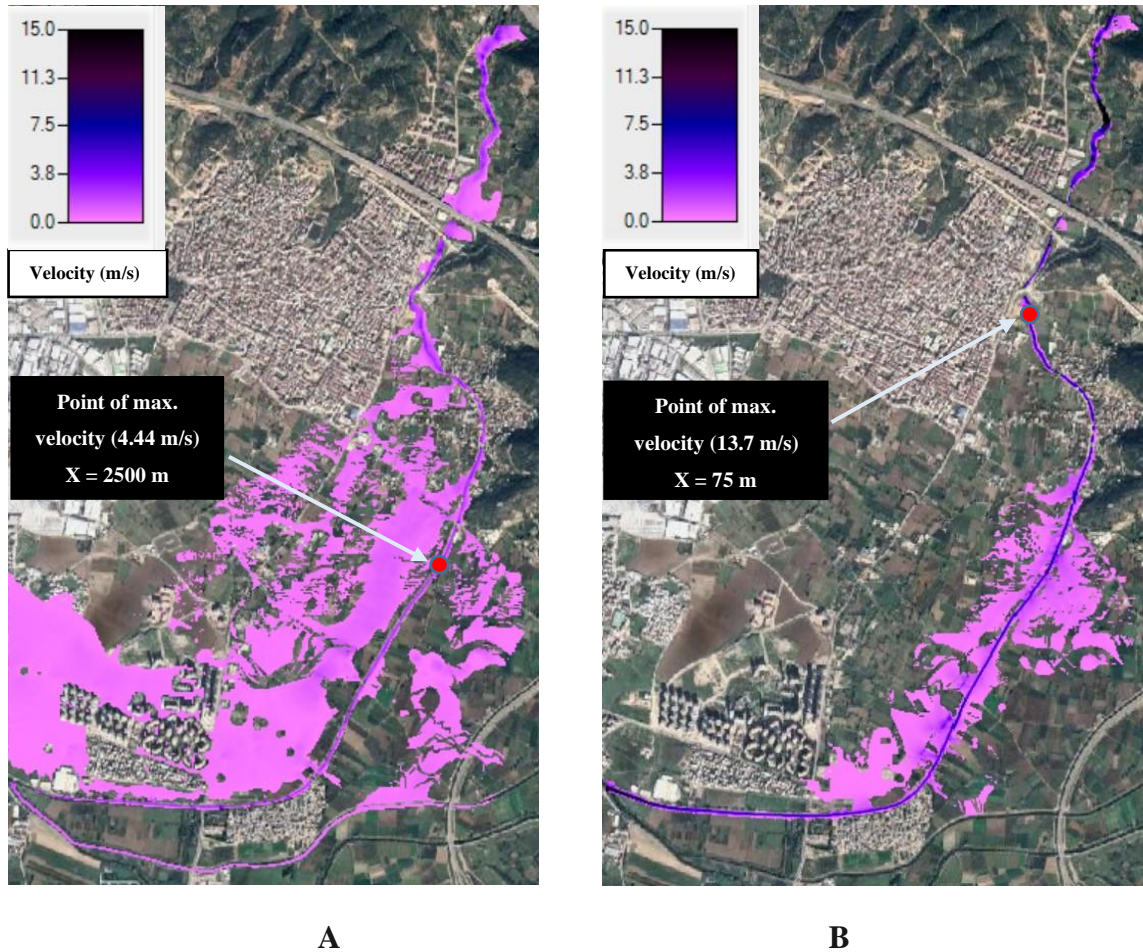


**Figure 4.7.** Velocity maps for  $Q_{500}$  **A)** before rehabilitation **B)** after rehabilitation

Before rehabilitation, a maximum velocity of 4.44 m/s was observed at  $X = 2500$  m in the main channel. High velocity of flow in a natural river bed would result in erosion of soil and deformation of the bed. After rehabilitation, a maximum velocity of 13.7 m/s at  $X = 75$  m was observed in the main channel. Thus, the velocity of flow in the main channel was much less before rehabilitation as compared to the case of after rehabilitation. This was observed due to the fact that the main channel before rehabilitation retained less water with high overflow. However, for the overbanks, velocity was observed to be higher before rehabilitation and lower after rehabilitation. This can also be attributed to the fact that there was high overflow before rehabilitation. Hence, it can be said that not only did the rehabilitation of channel decrease the overflow but also the decrease in velocity of overflow after rehabilitation reduced the risk of soil erosion near the banks.

Figure 4.8 shows the comparison of velocity maps for  $Q_{1000}$  before and after rehabilitation of Ismetiye creek.

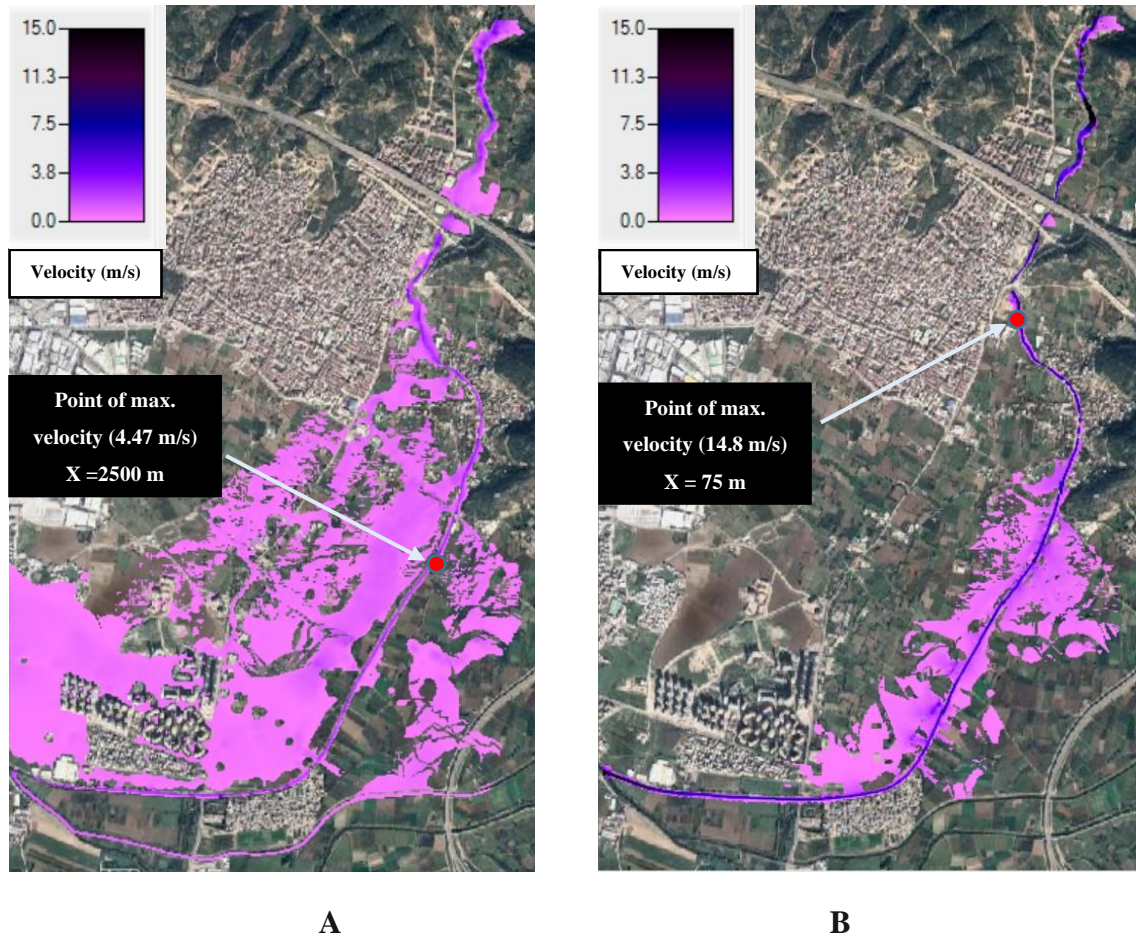


**Figure 4.8.** Velocity maps for  $Q_{1000}$  **A)** before rehabilitation **B)** after rehabilitation

Maximum velocity of 4.47 m/s was observed at  $X = 2500$  m in the main channel before rehabilitation. After rehabilitation, a maximum velocity of 14.8 m/s was observed at  $X = 75$  m. As compared to the maximum velocities obtained in the case of  $Q_{500}$ , the maximum velocities in the case of  $Q_{1000}$  were marginally higher. However, the locations of points of maximum velocities remained the same as that of  $Q_{500}$ .

Figure 4.9 shows the comparison of water surface elevation (WSE) before and after rehabilitation of Ismetiye Creek for  $Q_{500}$ .

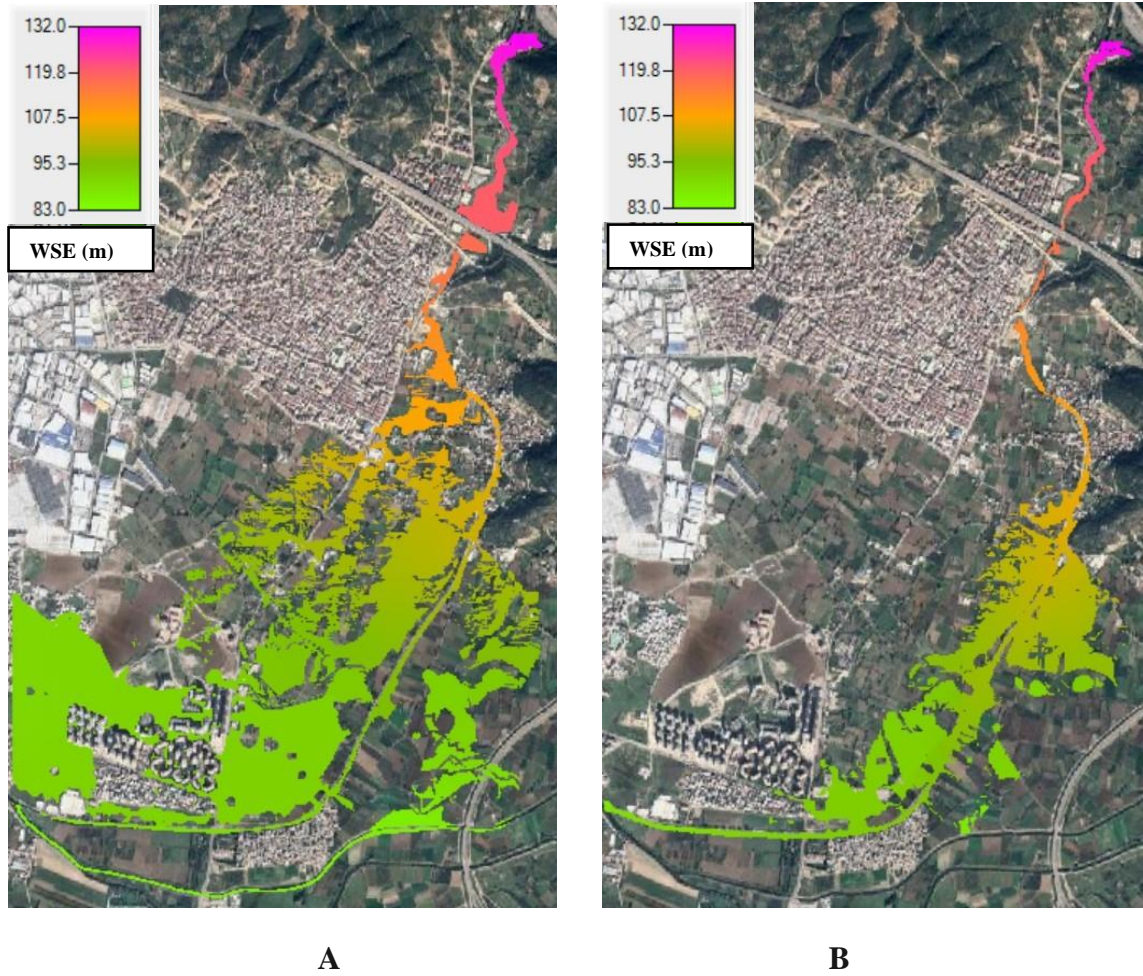


**Figure 4.9.** Water Surface Elevation maps for  $Q_{500}$  **A)** before rehabilitation **B)** after rehabilitation

Water surface elevation maps show the elevation of water surface from the sea level. Therefore, the elevation at a single point is the sum of elevation of terrain and water depth at that point. Both before and after rehabilitation, as we move from the upstream end to the downstream end, the elevation of the terrain decreases which subsequently results in the decrease of water surface elevation. Both before and after rehabilitation, the water surface elevation ranges between 132 m to 83 m from upstream end to downstream end of the channel. The slope of hydraulic grade line is 0.006.

Figure 4.10 shows the comparison of water surface elevation (WSE) before and after rehabilitation of Ismetiye Creek for  $Q_{1000}$ .

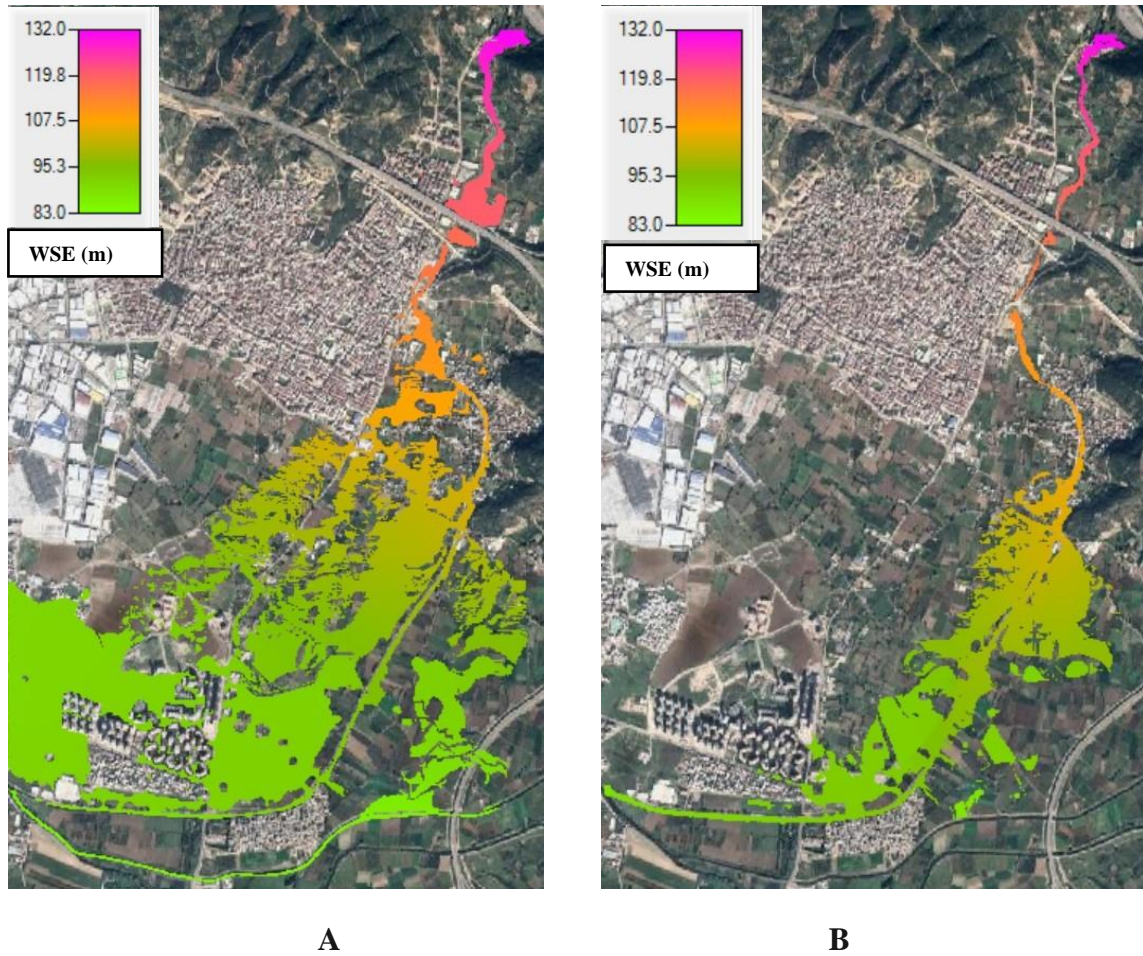


**Figure 4.10.** Water Surface Elevation maps for  $Q_{1000}$  **A)** before rehabilitation **B)** after rehabilitation

In case of  $Q_{1000}$  for both natural and rehabilitated channel, the water surface elevation also ranges between 132 m to 83 m from upstream end to downstream end of the channel. The slope of hydraulic grade line is 0.006.

Flood hazard maps were created to compare the risk of floods before and after the rehabilitation of Ismetiye creek. Flood risk zones as per the guidelines of Federal Emergency Management Agency (FEMA) 2018 were defined as shown in Table. 4.1. The magnitude of flood hazard is calculated by Eq. (4.1) (FEMA 2018).

$$\text{hazard} = \text{depth} \times \text{velocity} \quad (4.1)$$

**Table 4.1.** Flood risk classification scheme (modified from FEMA 2018)

Hazard (m <sup>2</sup> /s)	Flood Risk	Hazard Rating
< 0.2	Very Low	0
0.2-0.5	Low	1
0.5-1.0	Moderate	2
1.0-2.0	High	3
> 2.0	Extreme	4

Hazard zones were assigned a hazard rating starting from 0 to 4 with 0 corresponding to very low risk zone and 4 corresponding to extreme risk zone.

Figure 4.11 shows the comparison of flood hazard zones before and after rehabilitation of Ismetiye creek for Q<sub>500</sub>.

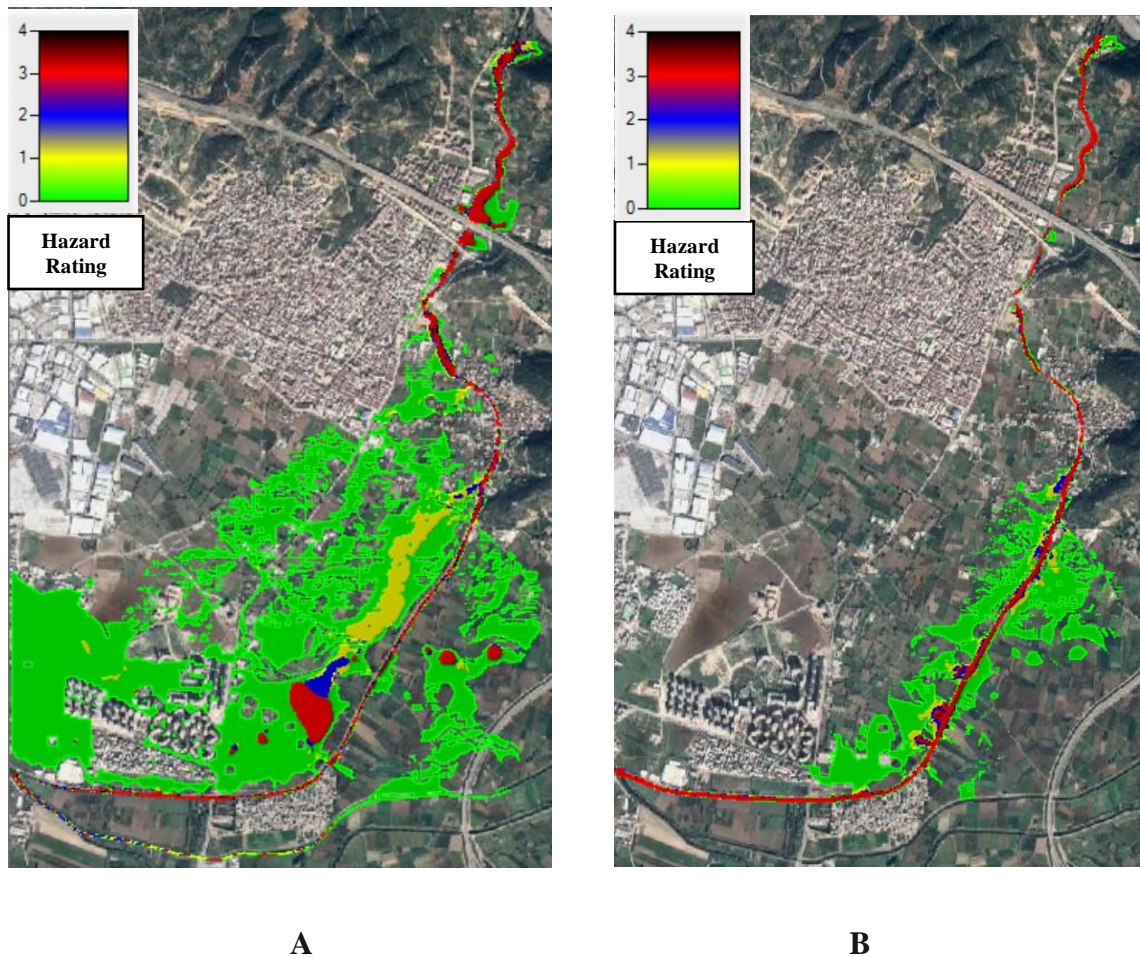


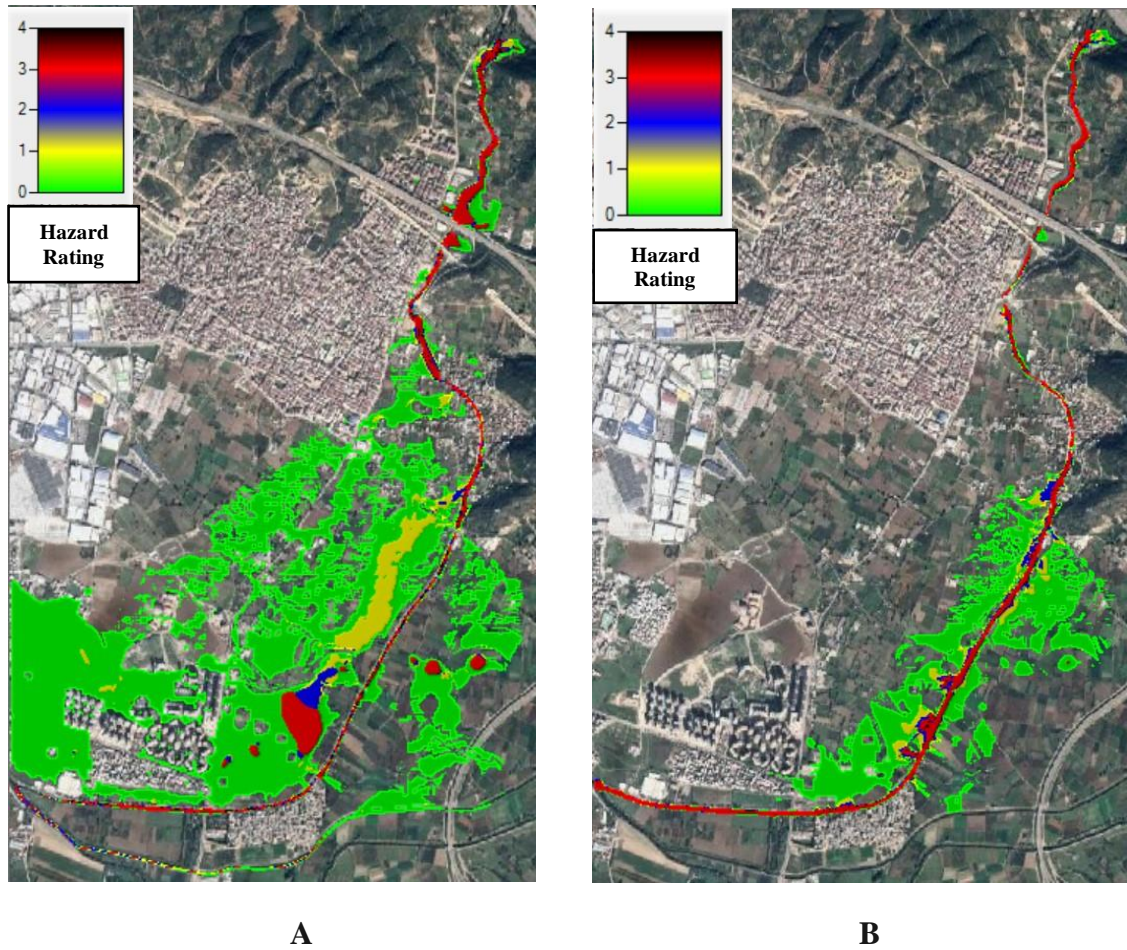
**Figure 4.11.** Flood hazard zones for Q<sub>500</sub> **A)** before rehabilitation **B)** after rehabilitation

From the hazard maps of natural channel and rehabilitated channel, it was observed that hazard rating was maximum inside the main channel taking the values 3 (high risk) and 4 (extreme risk) along the channel path.

The catchment area in case of natural channel was more prone to flooding as expected and the extent of hazard was more. On the right overbank side, there were traces of yellow, blue and red colors which correspond to a hazard rating of 1,2 and 3 respectively. The regions on right overbank side of Ismetiye with hazard rating of 2 (blue) and 3 (red) are in the vicinity of inhabited areas, making those areas susceptible to the danger of flooding.

However, after rehabilitation, the extent of hazard considerably decreased and a hazard map with green (hazard rating = 0) was observed throughout the catchment area except for the main channel and its immediate surroundings where some spots with yellow (hazard rating = 1) and blue (hazard rating = 2) were observed. However, these spots lie in uninhabited regions.

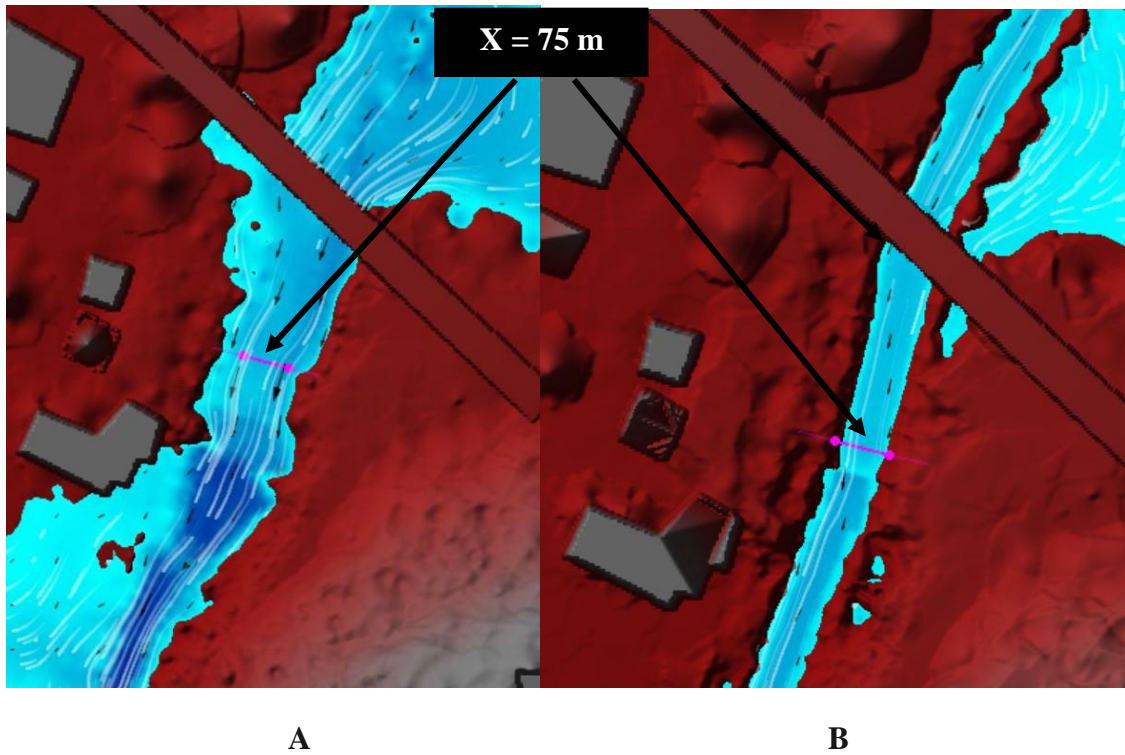
Figure 4.12 shows the comparison of flood hazard zones before and after rehabilitation of Ismetiye creek for  $Q_{1000}$ .



**Figure 4.12.** Flood hazard zones for  $Q_{1000}$  **A)** before rehabilitation **B)** after rehabilitation

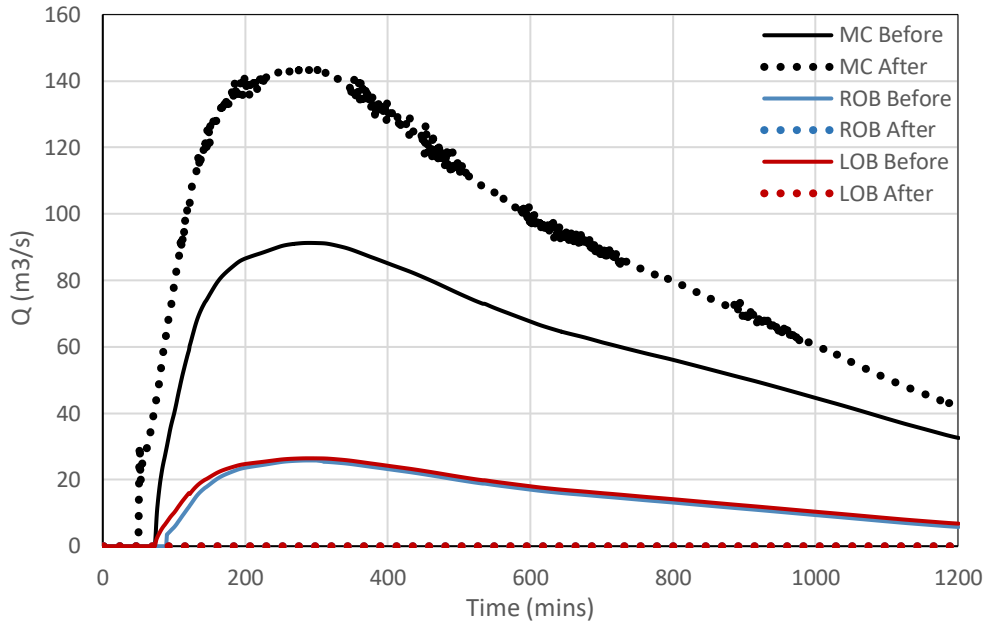
As expected, the extent of flood hazard was more in case of  $Q_{1000}$  as compared to that of  $Q_{500}$ . Due to high velocity of flow in case of rehabilitated channel, flood hazard was more near the banks as compared to the case of natural channel. Before rehabilitation, new settlements towards right over bank side of the downstream end of Ismetiye channel were exposed to inundations. However, there is no flooding seen in these areas after rehabilitation of the channel.

Cross-sectional lines were drawn at  $X= 75 \text{ m}$ ,  $1500 \text{ m}$ ,  $3000 \text{ m}$  and  $4000 \text{ m}$  along the channel in order to obtain flow hydrographs for  $Q_{500}$  and  $Q_{1000}$ . Separate lines were drawn for the main channel (MC) and each overbank. Therefore, hydrographs for the MC, right overbank (ROB) and left overbank (LOB) were calculated separately for each cross-section. Figure 4.13 shows the cross-section at  $X= 75 \text{ m}$  for  $Q_{1000}$ .



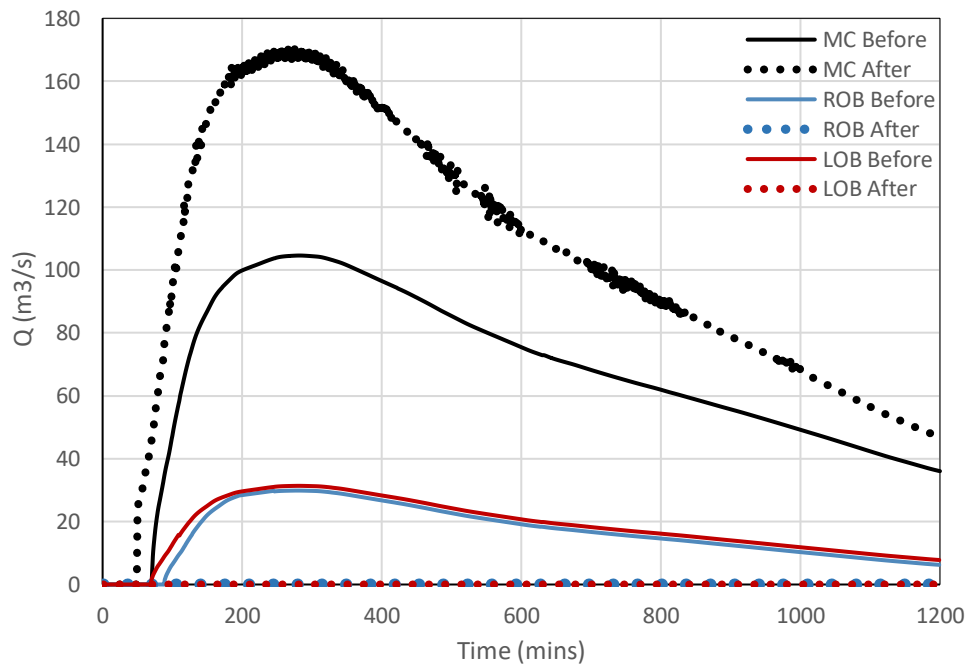
**Figure 4.13.** Cross-sections at  $X=75 \text{ m}$  for  $Q_{1000}$  **A)** before rehabilitation **B)** after rehabilitation

Flow hydrographs at  $X= 75 \text{ m}$  for  $Q=500 \text{ m}^3/\text{s}$  and  $Q=1000 \text{ m}^3/\text{s}$  are depicted by Figure 4.14 and Figure 4.15 respectively.



**Figure 4.14.** Flow hydrographs for  $Q_{500}$  at  $X=75$  m for main channel and overbanks

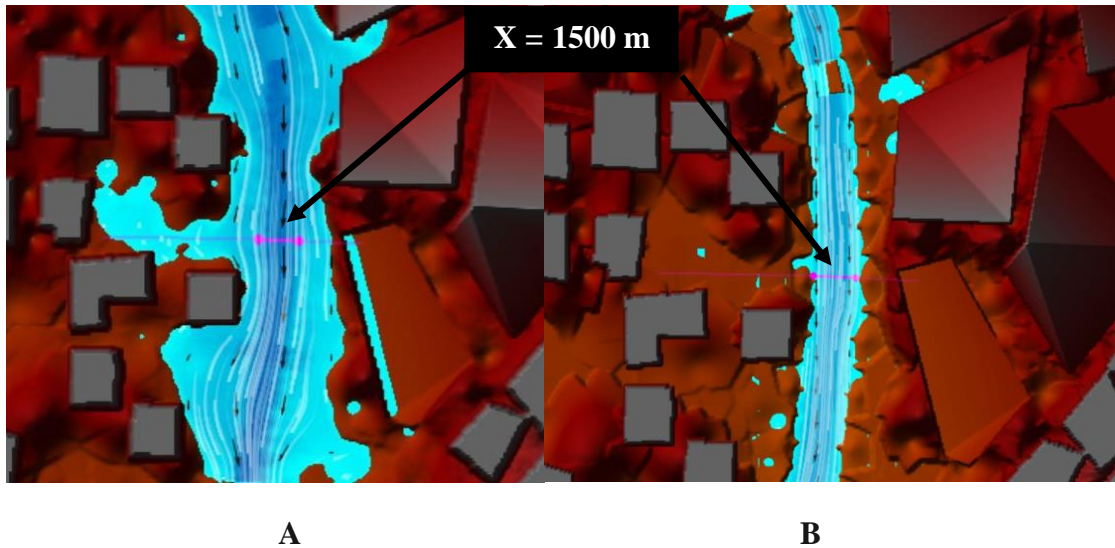
The peak in MC for  $Q_{500}$  before rehabilitation was attained at  $91.27 \text{ m}^3/\text{s}$  and after rehabilitation, it was attained at  $143.65 \text{ m}^3/\text{s}$ . There is a huge increase in the peak after rehabilitation, indicating that water was retained in the main channel. In the case of overbanks, no flooding was observed after rehabilitation which is attributed to the fact that there was no overflow from the main channel.



**Figure 4.15.** Flow hydrographs for  $Q_{1000}$  at  $X=75$  m for main channel and overbanks

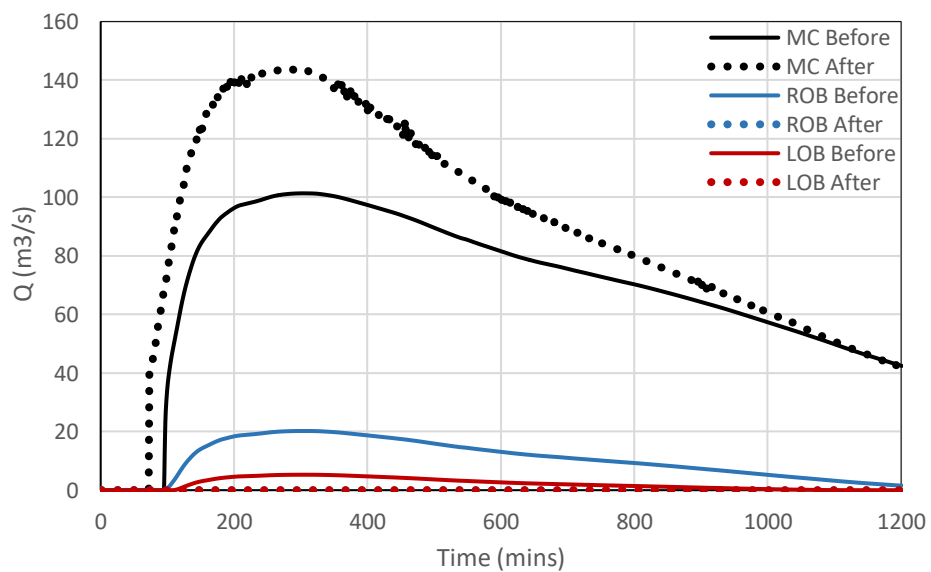
The peaks in MC for  $Q_{1000}$  were higher than those of  $Q_{500}$  as expected. The peak in MC before rehabilitation was attained at  $104.58 \text{ m}^3/\text{s}$  and after rehabilitation, it was attained at  $168.42 \text{ m}^3/\text{s}$ .

Figure 4.16 shows the cross-sections at  $X= 1500 \text{ m}$  with  $Q_{1000}$ .



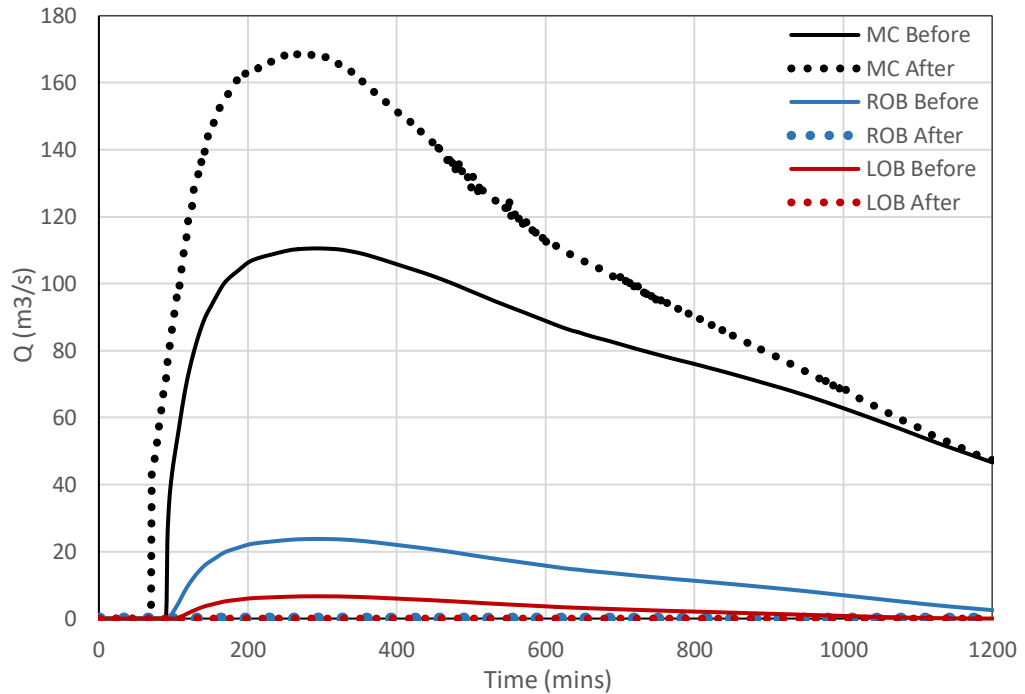
**Figure 4.16.** Cross-sections at  $X=1500 \text{ m}$  for  $Q_{1000}$  **A)** before rehabilitation **B)** after rehabilitation

Flow hydrographs at  $X= 1500 \text{ m}$  for  $Q=500 \text{ m}^3/\text{s}$  and  $Q=1000 \text{ m}^3/\text{s}$  are depicted by Figure 4.17 and Figure 4.18 respectively.



**Figure 4.17.** Flow hydrographs for  $Q_{500}$  at  $X=1500 \text{ m}$  for main channel and overbanks

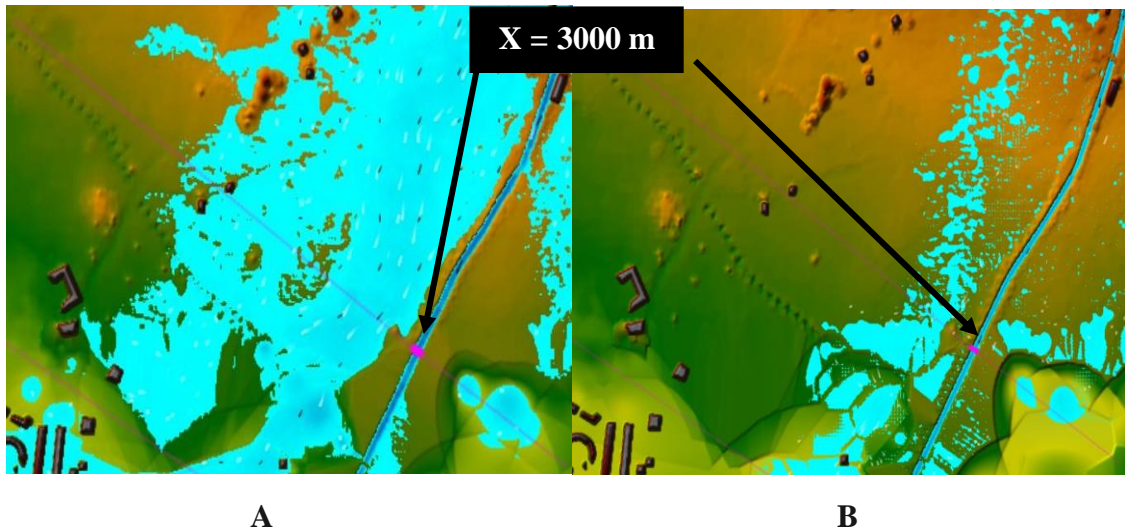
The peak in MC for  $Q_{500}$  before rehabilitation was attained at  $101.35 \text{ m}^3/\text{s}$  and after rehabilitation, it was attained at  $143.17 \text{ m}^3/\text{s}$ . Again, there is no overflow in the channel after rehabilitation.



**Figure 4.18.** Flow hydrographs for  $Q_{1000}$  at  $X=1500 \text{ m}$  for main channel and overbanks

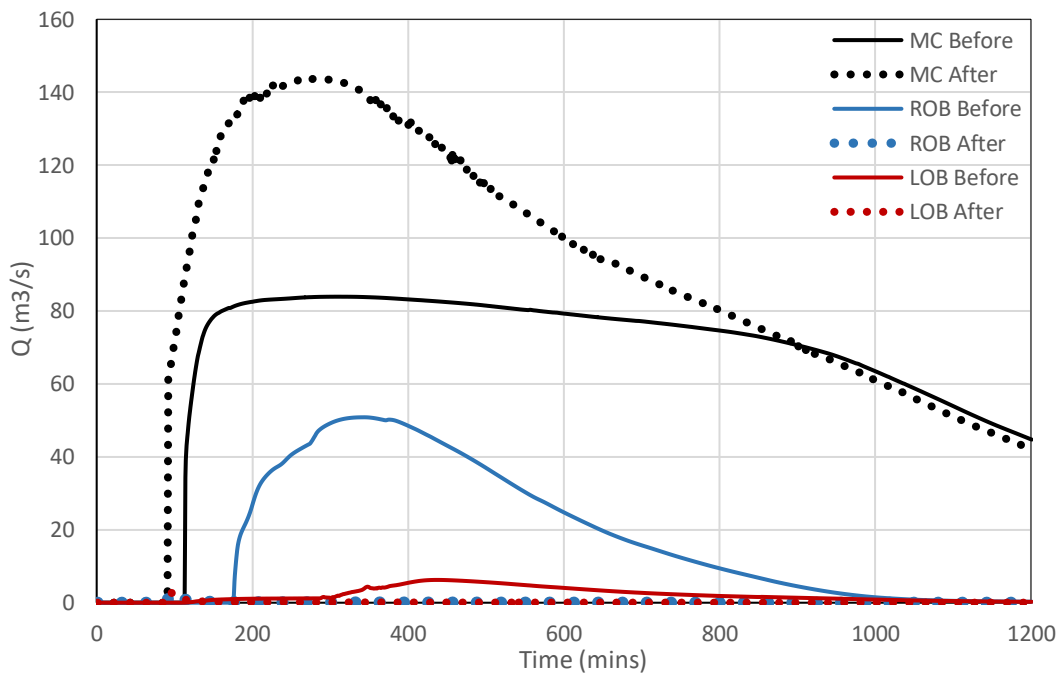
As expected, the peaks in MC for  $Q_{1000}$  were higher than  $Q_{500}$ . The peak before rehabilitation was attained at  $110.53 \text{ m}^3/\text{s}$  and after rehabilitation, it was attained at  $168.14 \text{ m}^3/\text{s}$ .

Figure 4.19 shows the cross-sections at  $X=3000 \text{ m}$  with  $Q_{1000}$ . The cross-sections here are much wider to cover the entire overbank flow.



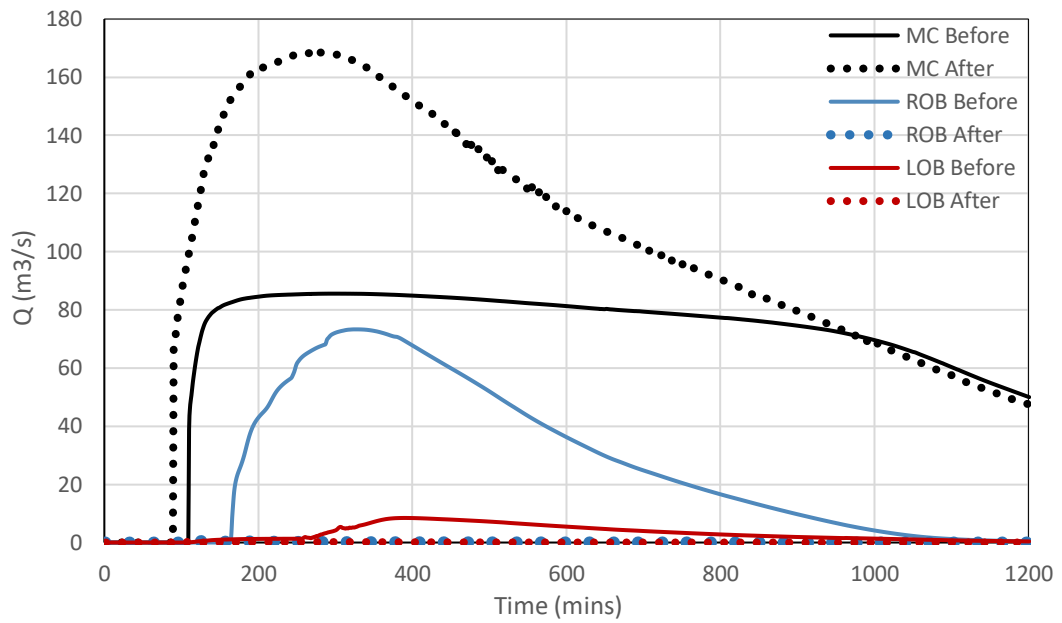
**Figure 4.19.** Cross-sections at X= 3000 m for  $Q_{1000}$  A) before rehabilitation B) after rehabilitation

Flow hydrographs at X=3000 m for  $Q=500 \text{ m}^3/\text{s}$  and  $Q=1000 \text{ m}^3/\text{s}$  are depicted by Figure 4.20 and Figure 4.21 respectively.



**Figure 4.20.** Flow hydrographs for  $Q_{500}$  at X=3000 m for main channel and overbanks

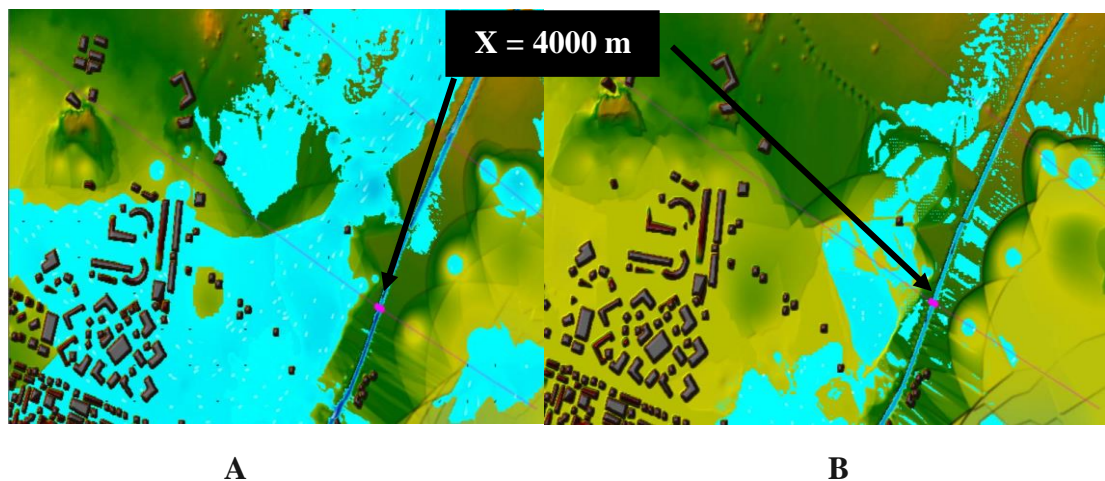
The peak in MC for  $Q_{500}$  before rehabilitation was attained at  $83.9 \text{ m}^3/\text{s}$  and after rehabilitation, it was attained at  $143.6 \text{ m}^3/\text{s}$ . There was no overflow in the channel after rehabilitation.



**Figure 4.21.** Flow hydrographs for  $Q_{1000}$  at  $X=3000$  m for main channel and overbanks

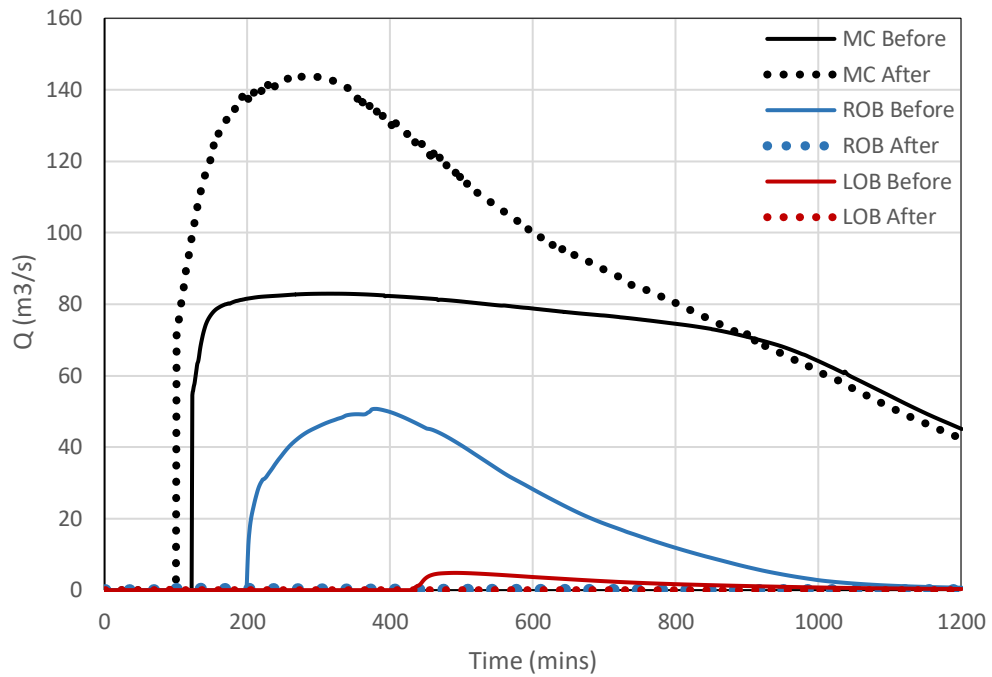
In case of  $Q_{1000}$ , the peak in MC before rehabilitation was attained at  $85.5 \text{ m}^3/\text{s}$  and after rehabilitation, it was attained at  $168.3 \text{ m}^3/\text{s}$ . For  $X=3000$  m, before rehabilitation, it was observed that the peak in MC was constant after a certain point. This indicated that maximum flow capacity of natural channel was reached.

Figure 4.22 shows the cross-sections at  $X=4000$  m for  $Q_{1000}$ . The cross-sections here are much wider to cover the entire overbank flow.



**Figure 4.22.** Cross-sections at  $X=4000$  m for  $Q_{1000}$  **A)** before rehabilitation **B)** after rehabilitation

Flow hydrographs at X= 4000 m for  $Q=500 \text{ m}^3/\text{s}$  and  $Q=1000 \text{ m}^3/\text{s}$  are depicted by Figure 4.23 and Figure 4.24 respectively.



**Figure 4.23.** Flow hydrographs for  $Q_{500}$  at  $X=4000 \text{ m}$  for main channel and overbanks

The peak in MC for  $Q_{500}$  before rehabilitation was attained at  $82.93 \text{ m}^3/\text{s}$  and after rehabilitation, it was attained at  $143.8 \text{ m}^3/\text{s}$ . There is no overflow in the channel after rehabilitation.

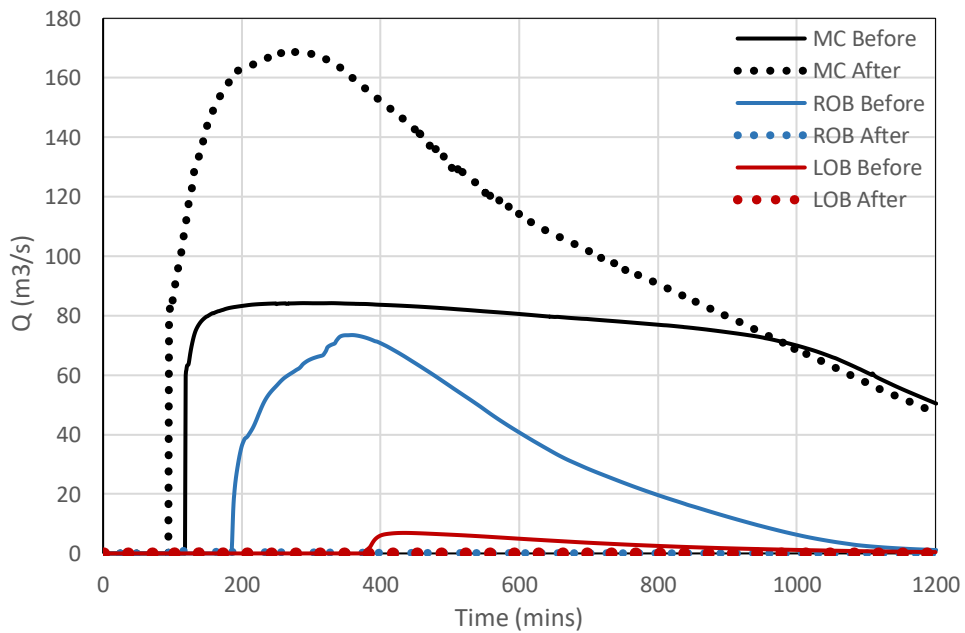


**Figure 4.24.** Flow hydrographs for  $Q_{1000}$  at  $X=4000 \text{ m}$  for main channel and overbanks

The peak in MC before rehabilitation was attained at 84.19 m<sup>3</sup>/s and after rehabilitation, it was attained at 168.6 m<sup>3</sup>/s. At X=4000 m, before rehabilitation, it was also observed that flow hydrograph peak was constant after a certain point. This indicated that maximum flow capacity of natural channel was reached. Table 4.2 and Table 4.3 show the peak discharge values for main channel and overbanks.

**Table 4.2.** Peak discharge values for natural and concrete channels in case of Q<sub>500</sub>

X (m)	Natural Channel			Concrete Channel		
	Q <sub>MC</sub> (m <sup>3</sup> /s)	Q <sub>ROB</sub> (m <sup>3</sup> /s)	Q <sub>LOB</sub> (m <sup>3</sup> /s)	Q <sub>MC</sub> (m <sup>3</sup> /s)	Q <sub>ROB</sub> (m <sup>3</sup> /s)	Q <sub>LOB</sub> (m <sup>3</sup> /s)
75	91.27	25.81	26.45	143.65	0	0
1500	101.35	20.21	5.27	143.17	0	0
3000	83.9	50.84	6.24	143.6	0	0
4000	82.93	50.71	4.82	143.7	0	0

**Table 4.3.** Peak discharge values for natural and concrete channels in case of Q<sub>1000</sub>

X (m)	Natural Channel			Concrete Channel		
	Q <sub>MC</sub> (m <sup>3</sup> /s)	Q <sub>ROB</sub> (m <sup>3</sup> /s)	Q <sub>LOB</sub> (m <sup>3</sup> /s)	Q <sub>MC</sub> (m <sup>3</sup> /s)	Q <sub>ROB</sub> (m <sup>3</sup> /s)	Q <sub>LOB</sub> (m <sup>3</sup> /s)
75	104.58	29.86	31.36	168.42	0	0
1500	110.53	23.77	6.64	168.14	0	0
3000	85.5	73.29	8.44	168.3	0	0
4000	84.19	73.45	6.91	168.6	0	0

Here is a generalization of results that can be concluded from the above graphs valid for both Q<sub>500</sub> and Q<sub>1000</sub>:

- It is obvious from the graphs that flow in main channel was more for rehabilitated case as compared to the natural case. This is because of the fact that channel capacity increased. The erosion of banks and deposition of sediments lowered the

channel capacity in natural river. This resulted in higher peaks of hydrographs at the shown sections across the main channel after rehabilitation.

- On the other hand, before rehabilitation, due to high overflow in the main channel, the peaks of flow hydrographs were comparatively lower.
- Likewise, for the overbanks, the flooding was more in case of natural channel as compared to the rehabilitated channel which is also reflected by higher peaks of flow hydrographs.

These results clearly indicate that the rehabilitation work of Ismetiye creek confined most of the flooding to the main channel preventing the overbanks from risk of inundation. Thus, it is safe to say that rehabilitation work on a channel in its natural state makes the catchment areas of the channel less prone to the risk of flooding.

## 5. CONCLUSION

### 5.1. Summary and Conclusion

In this research, the affect of rehabilitation on Ismetiye creek in Osmangazi, Bursa was thoroughly studied. The main aim of this study was to compare the flooding of Ismetiye creek before and after its rehabilitation. After rehabilitation of the creek, channel bottom was made of concrete and the sides of channel were made with stone walls. The rehabilitated channel was 4020 m in length. The cross-sectional width of rehabilitated channel ranged between 12 m to 18 m.

The main goal of modelling Ismetiye creek was to identify the difference in risk of flooding before and after its rehabilitation. The model for simulation was developed using ArcMap and HEC-RAS. Initially, elevation data obtained from BUSKI in the form of AutoCAD files was imported to ArcMap. Subsequently, this elevation data was used to create a DEM through IDW raster interpolation. DEM was then exported as a terrain to RAS Mapper menu of HEC-RAS. The terrain file was then modified by adding secondary channels, roadways, buildings and bridges over the main channel. 2D simulations were run for  $Q_{500}$  and  $Q_{1000}$  to obtain the flooding in catchment area.

As of 2022, Ismetiye creek was rehabilitated by BUSKI for a stretch of 4020 m leaving the remaining part of the creek in its natural state. However, the simulations were carried out assuming that the entire channel was rehabilitated. From the 2D simulations for both  $Q_{500}$  and  $Q_{1000}$ , it was found that Ismetiye creek before rehabilitation was more exposed to flooding with a high extent of water inundations as compared to the case of after rehabilitation. A maximum velocity of 4.8 m/s was observed for the main channel. Velocity on the overbanks was higher before rehabilitation which would result in erosion and deformation of the soil in case of flooding. Before rehabilitation, the overflow from main channel also reached the dry channel in the south of main channel resulting in the flooding of dry channel as well. From the results of simulations run for the natural channel, flood hazard was found to be significant for  $Q_{1000}$  but most of the catchment areas were found to lie in low-risk zone with a few exceptions where the flood risk was

high. However, these areas were found to be in agricultural land. With regard to risk of flooding in residential areas, Demirtas Barbaros, Doganevler and Cumhuriyet neighborhoods of Ismetiye creek catchment area were exposed to high water inundations.

On the other hand, the 2D simulations with  $Q_{500}$  and  $Q_{1000}$  for the rehabilitated channel showed decrease in flooding as the extent of water inundations reduced considerably. Also, there was no flooding in the south due to the overflow from main channel. For  $Q_{1000}$ , the maximum depth observed in the main channel was 5.120 m before rehabilitation and 5.794 m after rehabilitation. Thus, more water was retained in the main channel after rehabilitation, resulting in very less overflow which is also reflected by the flood hydrographs shown in the results for various sections. For instance, in case of  $Q_{500}$  at  $X=75$  m,  $Q_{MC}$  was found to be  $91.27 \text{ m}^3/\text{s}$  for natural channel while as it was  $143.65 \text{ m}^3/\text{s}$  for concrete channel. Thus, channel capacity increased for the concrete channel. Additionally, in case of  $Q_{500}$  at  $X=75$  m,  $Q_{ROB}$  was  $25.81 \text{ m}^3/\text{s}$  and  $Q_{LOB}$  was  $26.45 \text{ m}^3/\text{s}$  respectively, for the natural channel. However, for rehabilitated channel, these values were found to be  $0 \text{ m}^3/\text{s}$  due to no overflow.

The maximum velocity observed for the concrete channel was 14.47 m/s. Since most of the flow was retained in the main channel after rehabilitation, velocity of flow was very high for concrete channel as compared to the natural channel. After rehabilitation, a very small amount of flooding was observed in Ismetiye creek catchment area for both  $Q_{500}$  and  $Q_{1000}$ . The entire catchment area was found to lie in a very low risk flood hazard zone. All the inundated areas were found to be in the agricultural lands lying in close vicinity of Ismetiye creek. There was no risk of flooding at all for any of the residential areas lying in the vicinity of Ismetiye creek. Thus, it can be concluded that complete rehabilitation of Ismetiye creek by BUSKI will entirely remove the threat of flooding in the nearby residential areas.

## **5.2. Recommendations**

It should be again emphasized that only a stretch of 4020 m of Ismetiye creek was rehabilitated while the rest of the channel still remains in its natural state, leaving some

neighborhoods in Demirtas area of Osmangazi district like Doganevler and Cumhuriyet exposed to risk of floods.

Hence the following recommendations can be suggested to the environmental policymakers.

- Keeping the risk of minor flooding for the areas of Doganevler and Cumhuriyet neighborhoods in mind, completing the unfinished rehabilitation works of Ismetiye creek is essential.
- In case the rehabilitation work of Ismetiye creek is not completed, flood insurance schemes can be introduced for the residential neighborhoods which are susceptible to risk of floods.

## REFERENCES

- Abdessamed, D. and Abderrazak, B. (2019). *Coupling HEC-RAS and HEC-HMS in rainfall–runoff modelling and evaluating floodplain inundation maps in arid environments: case study of Ain Sefra city, Ksour Mountain. SW of Algeria*. Environmental Earth Sciences (2019) 78:586.
- Acosta, J., Keith, R., Hollite, J., Logronio, R., James, G. (2017). *Flood modelling using GIS and LiDAR of Padada River in south-eastern Philippines*. GISTAM 2017 - 3rd International Conference on Geographical Information Systems Theory, Applications and Management. 301-306.
- Astite, S.W., Belabid, N., Mahmoudi, N., (2015). *Cartography of flood hazard by overflowing rivers using hydraulic modelling and geographic information system: Oued El Harrach Case (North of Algeria)*. Revista de Teledeteccion, 44:67-79.
- Bricker, Jeremy, D., Schwanghart, Wolfgang, Adhikari, Basanta, R., Moriguchi, Shuji, Roeber and Volker. (2015). *Performance of models for flash flood warning and hazard assessment: The 2015 Kali Gandaki Landslide Dam breach in Nepal*. Mountain Research and Development, 37(1): 5-15.
- Bursahaber (2010). <https://www.bursahaber.com/bursayi-allah-korudu-makale,953.html>
- Chow, V.T. (1959). *Open Channel Hydraulics*. McGraw-Hill, New York.
- Climate Change Post (2022). River floods Turkey  
<https://www.climatechangepost.com/turkey/river-floods/>
- Fatih, S., (2013). *İsmetiye (kelesen) deresi islah uygulama projesi*. Mühendislik taşkın hidrolojisi raporu.
- FEMA (2018) *Guidance for Flood Risk Analysis and Mapping*. Federal Emergency Management Agency (FEMA), USA.
- Gary, W.B. (2020). *HEC-RAS river analysis system. 2D modelling user's manual*.  
<https://www.hec.usace.army.mil>.
- Gulbaz, S., Cevza, M., Aysenur.. Ugur. (2019). *Flood modelling of Ayamama River Watershed in Istanbul, Turkey*. J. Hydrol. Eng., 2019, 24(1): 05018026.
- Hashemyan, F., Khaleghi, M.R., Kamyar, M. (2015). *Combination of HEC-HMS and HEC-RAS models in GIS in order to Simulate Flood (Case study: Khoshke Rudan river in Fars province, Iran)*. Research Journal of Recent Sciences, 4(8): 122-127.
- Iglesias, (2014). *Flood disaster mitigation and river rehabilitation by Marikina City, Philippines*. Asian Disaster Preparedness Centre. <http://www.adpc.net.mz>

İsmail, H., Enes, Y., Fatih, O., İbrahim, D. (2021). *Comprehensive flood event specification and inventory: 1930–2020 Turkey case study*. International Journal of Disaster Risk Reduction, 56 (2021): 102086.

Lucien, H., Gebremeskel, S., Smedt, F., Hoffmann, L., Pfister, L. (2014). *Simulation of flood reduction by natural river rehabilitation using a distributed hydrological model*. Hydrology and Earth System Sciences, 8(6): 1129-1140.

Macrotrends (2020). Bursa, Turkey Metro Area Population 1950-2020  
<https://www.macrotrends.net/cities/22670/bursa/population>

Mondal, S. and Priyank, P. (2018). *Examining the utility of river restoration approaches for flood mitigation and channel stability enhancement: a recent review*. Environmental Earth Sciences (2018), 77:195.

Nataran, S. and Nisha, R. (2019). *An integrated hydrologic and hydraulic flood modelling study for a medium-sized ungauged urban catchment area: A case study of Tiruchirappalli city using HEC-HMS and HEC-RAS*. J. Inst. Eng. India Ser. A (June 2020) 101(2):381–398.

Neslihan, B. and Asli, K. (2020). *Flood hazard assessment of a flood-prone intensively urbanized area – A case study from Samsun Province, Turkey*. Geofizika, 37 (2020): 1–25.

Neslihan, B. and Asli, K. (2021) *Flood map production and evaluation of flood risks in situations of insufficient flow data*. Natural Hazards (2021) 105:2381–2408.

Rosgen, D. L. (1994). *A classification of natural rivers*. Catena, 22, 169-199

Sammen, S., Thamer, A., Quitiba, G. (2019). *Environmental consideration in flood mitigation and river restoration*. IOP Conf. Series: Materials Science and Engineering 518 (2019) 022088.

Tahmasbinejad, H., Feyzolahpour, M., Mehdi, M., Fatemeh, Z. (2012). *Rainfall-Runoff simulation modelling of Karun River using HEC-RAS and HEC-HMS model, Izeh District Iran*. Journal of Applied Sciences, 12(18): 1900-1908.

Thakur, B., Parajuli, R., Kalra, A., Ahmad, S., Gupta, R. (2017). *Coupling HEC-RAS and HEC-HMS in precipitation runoff modelling and evaluating flood plain inundation map Sacramento, California*. World Environmental and Water Resources Congress, 240-251.

USGS (2006). *Flood Hazards- A National Threat*. USGS Fact sheet 2006-3026,  
<https://pubs.usgs.gov/fs/2006/3026/2006-3026.pdf>.

WHO (2022). *Floods* -World Health Organization  
[https://www.who.int/health-topics/floods#tab=tab\\_1](https://www.who.int/health-topics/floods#tab=tab_1)

## RESUME

Name Surname : Amir Iqbal Wani  
Place and Date of Birth : Kupwara, Jammu and Kashmir, India,  
06/05/1996  
Foreign Languages : English, Turkish

Education Status  
High School (2011-2013) : Indira Memorial Jammu and Kashmir  
India  
VIT University, Tamil Nadu, India

BSc In Civil Engineering  
(2013-2017)  
Work Experience  
CAD Engineer (2017-18) : Dimension India Network, India

Contact (e-mail) : aamiriqbalwani@gmail.com

Publications : Study on strength characteristics of  
concrete using M Sand and Coconut Fibers  
IOP Conf. Series: Materials Science and  
Engineering Neeraja et al., 263 (2017)  
032014 doi:10.1088/1757-899X/263/3

A Comprehensive Study of Noise Levels  
from Vellore Town Tamil Nadu, using  
Mobile Applications  
Journal of Pollution Effects & Control,  
Muruganandam et al., J Pollut Eff Cont  
(2018),6:2DOI:10.4172/2375-4397.  
.1000218